Final Report

Open-Source High Flow Sampler for Natural Gas Leak Quantification

Colorado State University: Daniel Zimmerle
Timothy Vaughn
Kristine Bennett
Cody Ross

SLR International: Matthew Harrison
Aaron Wilson
Chris Johnson

Prepared for

California Air Resources Board

Contract: 19ISD010

Date: 04/14/2022

Disclaimer

The statements and conclusions in this report are those of the contractor and not necessarily those of the California Air Resources Board. The mention of commercial products, their source, or their use in connection with material reported herein is not to be construed as actual or implied endorsement of such products.

Executive Summary

High flow sampling remains the predominant method for measuring individual emission points. A High Flow Sampler (HFS) entrains the emissions in a stream of air and routes the combined flow through an instrument where flow and concentration measurements are used to compute the emission rate. Developed in the 1990s, the method is widely adopted, but the most prevalent commercial instrument for HFS measurements (Bacharach® HI FLOW® Sampler or "BHFS") is no longer manufactured. The California Air Resources Board (CARB) commissioned Colorado State University (CSU) and CSU collaborated with SLR International (SLR) to develop an open-source architecture for future instruments and, if possible, to encourage the development of new commercial products.

Open-source architecture: An architecture for an open-source high flow sampler (OS-HFS) was developed during the project. Key innovations were demonstrated, including:

- Selection and demonstration of next generation gas sensors, blower, and flow measurement sensors. Key issues with these subsystems were also identified, with advice for future users of the design. (Figure 1).

  No readily acceptable substitutes or improvements were found for the existing BHFS appurtenances, such as the hose, bag, and other emission collection equipment. The prototype continues with the BHFS supplied equipment.

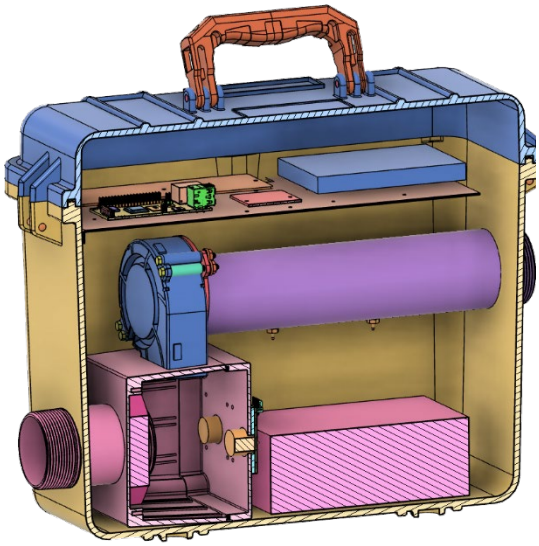

Figure 1: Cutaway view of the OS-HFS instrument design.

- The OS-HFS demonstrates the concept of a sensor-flexible *high flow platform* that could adapt to new uses and challenges as they arrive. This architecture is achieved by isolating computation and display elements from sensing and blower elements. A commercial, off-the-shelf, single board computer (SBC) was used for computation and display. The SBC communicated to all sensors via industry-standard serial protocols. This architecture isolates the computer, data interfacing, human interface, battery management, and similar supervisory systems from the sensor systems.

  Adopting this approach will make high flow instruments more adaptable as needs change and expectations for data handling and communication evolve.

- To the extent possible, the OS-HFS utilized open-source or easily sourced components, making the system accessible to anyone interested in constructing a copy or using the

design as the basis for a productized instrument. This includes use of platform-independent Python coding for all software, readily accessible sensor components, and use of a commercial high-volume blower used in another application (computers).

- Illustrating a new package design that fits better with in-field experience than the backpack packaging of the BHFS. Improvements include an improved graphical user interface, better placement of the user interface, smaller instrument size, and longer and more stable battery life. (Figure 2)

Figure 2: Integrated OS-HFS instrument during initial Testing.

The prototype demonstrates the concept of a sensor-flexible *high flow platform* that could adapt to new uses and challenges as they arrive. Section 5.1 provides additional detail summarizing the new open architecture.

Testing pre-production HFS instruments: The project also tested three additional pre-production HFS instruments under development by three different companies. Testing indicates that these units should be capable of replacing the current BHFS when completed.

Certain features of the CSU prototype were represented in some of the pre-production instruments, such as:

1) Modernized user interface and data collection. For example, several pre-production units added remote displays that were not tethered to the unit, and all provided some amount of data logging.

2) Two of the pre-production units utilized smaller packages that were more readily positioned by an operator during measurement, while one closely mimicked the BHFS backpack configuration.

3) Despite usability progress, field use and associated ergonomics remain challenging: All the instruments – CSU prototype included – are still bulky and heavy for use in the field, particularly since no unit identified more compact or lighter weight hoses and enclosures for capturing the leak.

However, none of the instruments included several key elements identified during this work (see Section 5), most importantly, support for multiple complementary sensors. Field experience

indicates that it is operationally challenging to correct for varying gas mixtures in field conditions. The CSU prototype included one sensor as the primary measurement sensor and a second sensor to detect changes in gas mix, even if a composition-dependent correction was not possible without more information. The pre-production units were either methane-specific or utilized combustible gas sensors, like the BHFS.

Additionally, pre-production units should undergo testing similar to what was conducted here prior to field use. All units exhibited problems of some nature – all likely fixable – but additional testing would raise confidence in these instruments for future use.

High flow method and instrument testing: Incidental to the main project goals, the project performed extensive testing of the high flow method in a range of conditions.

Controlled-release testing on realistic equipment at CSU's Methane Emissions Technology Evaluation Center (METEC) indicates that uncertainties for high flow measurements *independent of any instrument* are likely underrepresented in current literature, analysis, and reporting. Testing with the CSU prototype, one commercial instrument, and three pre-production instruments indicated substantially more variability and error in measurement results on realistic equipment than was seen when emissions were introduced directly into the instrument. These results indicate that user practices and environmental conditions may contribute substantial uncertainty to component-level measurements. Characterization of these uncertainties and development of measurement best practices are advised.

Additional notes: The high flow method remains one of the few methods suitable for isolating individual emission points for direct measurement. Quality instruments that will play a key role in characterizing leak rates for many years to come are near completion.

Contents

Table of Figures

1. Introduction

1.1 Project Context and Objectives

Accurate source emission measurement is key to many efforts by the California Air Resources Board (CARB), as well as industry efforts to understand and reduce emissions. CARB, NGOs[1–5], and the US Department of Energy (DOE)[6–8], have sponsored research programs to understand natural gas emissions. These field efforts have often used direct emission rate measurement techniques to obtain an accurate characterization of emissions at the component level on a diverse range of facilities from production and exploration through distribution. Ultimately, CARB is most interested in mitigation of emissions. Practical implementation of mitigation programs often requires pre- and post-mitigation emission measurements.

Figure 3: High flow instrument in use. Blue fabric encloses the leak source.

Whether for research or mitigation, measurement of component emissions is most often completed using the high flow measurement method using a purpose-built instrument: A *High Flow Sampler* (HFS). Despite the varied needs and uses, there is now no commercially available HFS instrument. The most prevalent commercial instrument for HFS measurements to date (the Bacharach® HI FLOW® Sampler or "BHFS"), a 1990s design, was discontinued by its manufacturer 2 years ago. At a time when demand for measurement is growing, the devices are now unavailable.

1.1.1 High Flow Sampling in the Context of Other Methods

While downwind techniques, such as tracer-flux [9,10] or mass balance techniques [11], can estimate emissions at the facility level, corrective action typically requires detection and measurement at the component level. In addition, measurements of component-level emission sources are needed to inform operators' emissions mitigation programs. Regulatory programs are most interested in emission rates by component or process to better target emission reduction programs and to perform cost/benefit assessments. All these efforts require measurement using a qualified, standardized device and an associated measurement protocol for its use.

The scientific and industry standard for this type of measurement is the HFS, originally developed in the 1990s [12]. This instrument has achieved regulatory acceptance and is routinely utilized for scientific studies [1–3,13–15], internal industry emission surveys, and regulatory reporting[16]. In recent years, a typical process is to detect leaks using optical gas imaging (OGI) or US Environmental Protection Agency (EPA) Method 21[17], and then subsequently quantify those leaks using an HFS. Only when an HFS does not work (e.g., leak is too large) do teams resort to other leak measurement methods, such as in-stream anemometers or anti-static bags[18].

In brief, to use an HFS instrument, the operator loosely encloses the emission point. A blower in the HFS instrument then draws both the entire leak and surrounding air through the instrument and across sensors which measure both the concentration (% gas by volume) of the target gas species (e.g., methane or volatile organic compounds (VOCs)) and the total volume of air flow. A second sensor measures the background concentration of the same gas in surrounding air. Mass flow of the target species is calculated from the overall mass flow, background concentration, and emission-point concentration.

In summary, while many instruments are available to identify emission locations (optical gas imaging, gas sniffers, laser-based detectors), and many instruments can produce an estimate of the concentration of the target species in air (ppm, or ppm-m readings), the only widely accepted, general method to quantify emissions from components is high flow sampling.

1.1.2 Current Market Situation for HFS Instruments

While the technique is simple and well understood, the only commercially available instrument, the BHFS [19], has recently been discontinued. Many existing BHFS instruments are still in use, but long-term support is uncertain. The instrument has faced several challenges due to its usability (weight, bulk, potential lack of intrinsic safety) and concerns about its accuracy when utilized with wet gas[20–23].

Recent studies (spring 2019) have further illuminated problems with the BHFS. The *National Physical Laboratory* in the UK analyzed the instrument's sensors in a recent paper[24] and highlight several software and sensor performance issues. CSU also performed extensive testing in spring 2019 [25] using the gas mixing and flow control capabilities at the *Methane Emissions Technology Evaluation Center (METEC)* at CSU. These tests revealed several previously undocumented issues with the instrument, including variations in indicated emissions with total flowrate through the instrument, and changes in indicated emissions when switching from high-to-low, or low-to-high, gas concentrations. A recent field campaign [26] paired a subset of BHFS measurements with concurrent SUMMA-canister samples and found poor correlation in the so-called transition zone between concentrations where the sensor operates in catalytic oxidation mode and thermal conductivity mode – an indicated leak hydrocarbon concentration of 3-6 %. The instrument failed to transition even though efforts were made to minimize the use of practices known to cause this unwanted behavior.

Several implementations of high flow systems have been developed for specialized circumstances, including measuring emissions larger than the BHFS capacity[27]; measuring small, distributed emissions[28]; measuring emissions from underground pipeline leaks[3]; and measuring emissions using the "dynamic chamber" method[29,30]. Each of these developments has resulted in much larger instrumentation sets, typically vehicle mounted, and often using laboratory-grade instruments to provide the necessary sensor resolution. In October 2017, EPA's Office of Research and Development (EPA/ORD), in conjunction with EPA Region 8, were awarded funding of $100,000

through the EPA Regional Applied Research Effort program to develop and bench test components of an HFS prototype [23].

In summary, when this project started, no new commercial instruments were under development. Revision or redevelopment of an HFS has been impeded by the expected small lifetime volume (≈1500 units over 20 years*) and required development cost. While several scientific groups have developed their own one-off HFS instruments, none of these designs represent a reproducible, compact, or standardized design necessary for practical deployment and widespread use. A practical, reliable, compact, and versatile version of an HFS instrument is necessary to achieve widespread use and acceptance of results, and is critically needed for industry, governmental and scientific purposes.

Several technological advances since the 1990s are now available and can improve the operation and packaging of future HFS instruments:

- Gas concentration sensors have advanced substantially since the 1990s, including sensor-internal analog-digital (A/D) conversion, new sensor elements, and higher sensitivity.
- Auxiliary sensors for flow, power supply monitoring, and other purposes have both advanced and decreased in cost since the 1990s.
- Computer control of air flow (i.e., blower speed) is more practical using readily available speed controllers, including controllers internal to the blower assembly itself.
- Computational and computer memory improvements now support time series logging of sensor readings for quality assurance, method requirements (e.g., ensuring stabilized readings), and capturing changing emissions.
- Current lithium batteries provide more compact and stable power supplies than were available in the 1990s.

1.1.3 Project Objectives

The stated objectives of this project were to develop an open-source design that reduces the risk of producing a new product generation, i.e., for a commercial entity to develop a new HFS instrument.

Project deliverables were:

1) Designs for key components which are not currently available off-the-shelf.
2) Consider designs that retrofit existing instruments with improved sensors and electronics – if retrofits emerge as a viable path forward.
3) Pre-production software embodying the method and quality control.
4) Recommended component selection or design for intrinsic safety.
5) Sourcing and construction instructions to build the instrument.

* Estimate based upon anecdotal data from private conversations with a company distributing BHFS units over the last decade. Estimate does not necessarily account for any increasing interest in methane emissions mitigation due to regulatory, company, or certified gas programs.

Note that the open-source design would still require additional product development and safety certification to become a saleable instrument.

During the project, several commercial entities announced plans to develop new HFS instruments. Drivers for this sudden increase in commercial interest are unclear but are likely due to increased interest by operators and regulators in replacement instruments for the BHFS. It is also possible that this project both stimulated additional interest and helped companies identify HFS instruments as a commercially viable opportunity. By spring 2021, it was increasingly clear that the commercial efforts would arrive on market near the end date of this project. Therefore, the project team engaged with three manufacturers and tested each of their pre-production units using the same protocol used for the prototype OS-HFS being developed herein. The incumbent BHFS was also included in testing as a point of comparison for all instruments under development.

1.2 Organization of This Report

Chapter 2 provides an overview of the high flow method, including a qualitative summary of potential error sources in the method and in instruments used for the method. Chapter 3 describes the OS-HFS design created by this project, with emphasis on selection and evaluation of key instrument components. Chapter 4 summarizes prototype testing and Chapter 5 provides conclusions and recommendations for the high flow method and instruments. Appendices provide auxiliary written information. Test data, software, mechanical design, and PCB layouts for the OS-HFS are included in attached files.

1.3 The Technical Advisory Panel

The project also included a Technical Advisory Panel (TAP) to review progress of the project. The TAP included approximately 50 contributors in the oil and gas arena, including representatives from oil and gas companies, methane detection technology companies, and regulatory agencies. The panel met several times via Zoom or Teams in the early stages of the project in 2020 (April 16th, May 21st, June 29th) to discuss options for blowers, sensors, and other design elements desired in a next-generation HFS.

Subsequent meetings in 2021 (January 20th, July 14th) and 2022 (March 29th) provided updates on progress, presented prototype information, and solicited feedback from the TAP. These meetings occurred via Teams. Additionally, the project team met with several of the TAP members on an individual basis to get more detailed input and understand the needs and desires of the likely customer base.

Two members of the project team also participated in a “customer discovery” process during early 2021 that solicited feedback from HFS users, potential suppliers, and other groups. Learnings from these stakeholders impacted the OS-HFS design in many tangible and intangible ways.

2. Overview of the High Flow Method

2.1 Method Description

The high flow method quantifies the flow rate of an emission source (Q_{CH_4}) by entraining it completely within a flow stream and simultaneously measuring the flowrate of the total stream ($Q_{hfs} = Q_{CH_4} + Q_{air}$) and the concentration of the emission (C_{CH_4}) entrained. The two measured parameters are then used to calculate the unknown flowrate of the emission source, as given in equation set (1).

$$C_{CH_4} = \frac{Q_{CH_4}}{Q_{CH_4} + Q_{air}}$$

$$Q_{CH_4} = C_{CH_4}(Q_{CH_4} + Q_{air})$$

$$Q_{hfs} = Q_{CH_4} + Q_{air}$$

$$Q_{CH_4} = Q_{hfs} C_{CH_4} \qquad (1)$$

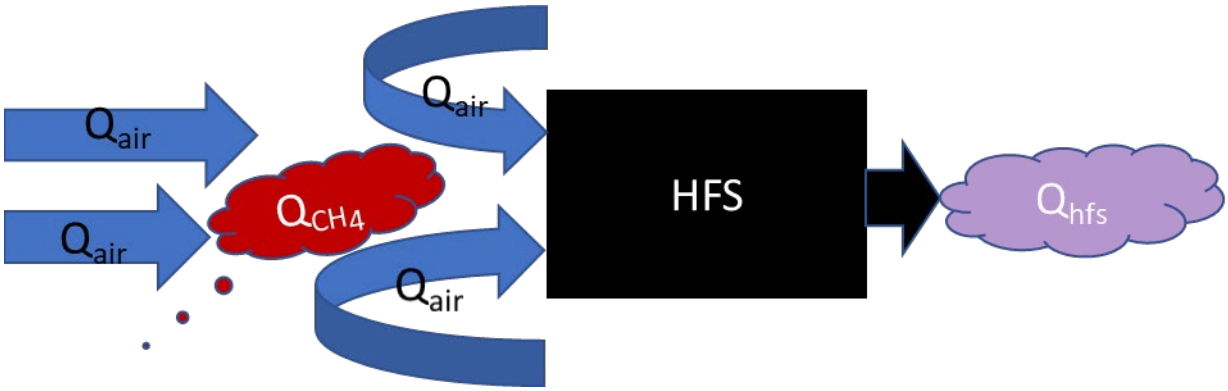

Figure 4: A high flow sampler (HFS) quantifies the flowrate of an emission source directly by entraining the emission source (Q_{CH4}) completely within a bulk flow of surrounding air (Q_{air}) and measuring the concentration of the emission species within the total flow through the HFS (Q_{hfs}).

The following assumptions are intrinsic to the method:

- That the air and methane behave as ideal gases.
- That the air and methane are perfectly mixed.
- That the concentration measurement is perfectly accurate from 0-100 %.
- That the flow stream measurement is perfectly accurate over its defined usage range ($Q_{hfs,min}$ to $Q_{hfs,max}$), and unaffected by the relative proportion of air/methane.
- That the emission source is entrained completely by the flow stream. This implies that Q_{CH4} must be <= $Q_{hfs,max}$.

It is also important to note that concentration measurements made by instruments vary in the specificity of gas sampled. While some units may use sensors that are sensitive only to methane, other instruments utilize sensors that are more generally sensitive to all hydrocarbons, or potentially to all combustible gases.

Figure 5: A BHFS is used to measure an emission on a wellhead.

The archetype commercial offering for natural gas component leak quantification has been the BHFS shown in use in Figure 3 and Figure 5. A blower contained within the backpack creates the flow stream drawing in the emission source and excess air. In both Figure 3 and Figure 5, the operator has used the bag attachment to help block the wind and direct the emission into the BHFS. The bag is draped loosely to avoid restricting flow to the BHFS and allow excess air to be drawn in and mixed with the emission source. Sensors inside the backpack measure the gas concentration and report the measured flow, measured concentration, and calculated emission rate to a hand-held screen. The results can also be stored as text data and retrieved over a computer interface.

An HFS could be constructed in a variety of ways, and several groups have implemented their own versions using different techniques for flow and concentration measurements (see [27,31]). Other approaches are also possible. The configuration of a specific HFS would be guided by the application of interest, usage model, required accuracy, desired cost, safety concerns, available resources, and other factors.

Converting the principles of this simple method into a useful, real-world measurement device is non-trivial and subject to potential limitations and sources of error, some of which are discussed in the following sections.

2.2 Sources of Instrument Error

Gas composition, cross sensitivities, sensor saturation, and sensor poisoning can all contribute to errors in readings reported by HFS instruments. Environmental effects such as temperature, pressure, and relative humidity may also influence reported results. Properly accounting for each of these factors and specifying the appropriate (and inappropriate) use cases for the instrument can solve most of these issues, either by design or procedural approaches.

Gas composition and typical emission rates will vary greatly across the natural gas supply chain along with environmental conditions. For example, using an HFS instrument with a methane specific detector to measure tank thief hatch emissions may provide an accurate methane emission rate but will likely under report the whole gas emission rate and give an inaccurate picture of VOC

emissions present. Depending on the end goal of the measurement this may or may not be problematic.

2.3 Potential Method Errors

Two potential shortcomings of the high flow method are incomplete capture and "over-capture":

Incomplete Capture may occur when attempting to capture a source where:

- The flowrate is larger than the HFS instrument is capable of measuring.
- An emission source has an exit velocity that cannot be overcome by the HFS blower.
- Wind disperses the emission source such that the HFS blower cannot entrain the emissions.
- Enclosure of the emission source is incomplete, and some emissions are emitted outside the enclosure and not entrained into the instrument.

Practitioners can guard against incomplete capture by observing the measurement with an OGI camera to ensure that all visible emissions are entrained into the instrument.[25]

Over Capture occurs when the motive flow of the HFS withdraws an emission at greater than its natural emission rate, effectively sampling "stored emissions" rather than "emission rate." Over capture may occur when insufficient dilution air is admitted along with the emission source and the HFS effectively "vacuums" the source from its containing vessel. While this error may occur in a number of situations, it is most prevalent when measuring openings on tanks, i.e., when sampling a large volume of stored emissions at near-atmospheric pressure.

3. Open-Source Design of a High Flow Sampler

The CSU prototype open-source high flow sampler (OS-HFS) was meant to be a replacement for the BHFS that addressed that instrument's shortcomings, expanded its capabilities, and refreshed component selection for long-term supportability. Performance targets for the OS-HFS were guided by the specifications of the BHFS as a baseline. The project sought to reproduce the general functionality and maintain the existing usage model of the BHFS but with improved performance and user experience. Overall goals were to:

- Reduce the size and the weight.
- Improve battery performance.
- Expand the lower and upper ends of the measurement range.
- Improve overall system accuracy.

Preliminary designs showed that this would be possible with careful selection and integration of appropriate off-the-shelf components.

3.1 Architecture and Key Components

3.1.1 Mechanical Architecture

This section provides an overview of the electronic and mechanical architecture of the instrument. The mechanical architecture of the instrument was designed for a specific usage model, based upon field experience of the project team in prior projects [1,2,25,26].

Previous instruments: The BHFS packaged the instrument into a metallic box placed in a backpack for ease of carrying. While the backpack could potentially hold some attachments for the instrument, there was generally insufficient space in the backpack for the hose and larger capture equipment. As a result, the operator(s) would need to make multiple trips to bring equipment to each leak. Additionally, field experience indicates that, in actual use, the operator typically placed the backpack on the ground, placed the display in a convenient position using the magnetic attachment, and then arranged inlet equipment to capture the leak (Figure 5). The team's field experience indicated that the backpack design was not well suited to practical field conditions. The backpack is difficult to clean and picks up dirt and oil from the surrounding area. Attachments likewise become dirty, and it is problematic to place these in the backpack with the instrument. Finally, the cord and display, while often convenient, were also inconvenient to stow and, in many cases, could not be magnetically attached near the point of measurement. In practice, many field teams utilize two operators for high flow measurements; one to enclose the emission source, and one to monitor and record the data from the HFS display.

Current design: The mechanical architecture of the OS-HFS is based upon the following use model:

- Move instrument and required attachments near the leak.

- Place instrument unit on a nearby surface and open lid.
- Arrange collection attachments (hoses, bags, etc.) to capture the leak.
- Monitor the display screen to initiate and record the measurement.
- Remove attachments, close lid, move to next measurement location.

To move the instrument, a shoulder strap may be fitted to the instrument and swung over one or both shoulders to free up hands for carrying other equipment; plastic case components are utilized to minimize the instrument weight. While not completed in the current prototype, case components may need to be spray-coated with a conductive metallic finish to improve grounding and reduce static discharge.

Figure 6 provides a schematic cutaway view of the OS-HFS. Principal components are labelled. A cosmetic cover enclosing the electronics and display on the top shelf was not designed and is not shown. The prototype uses a Pelican™ Pelicase™ 1430 as a case.

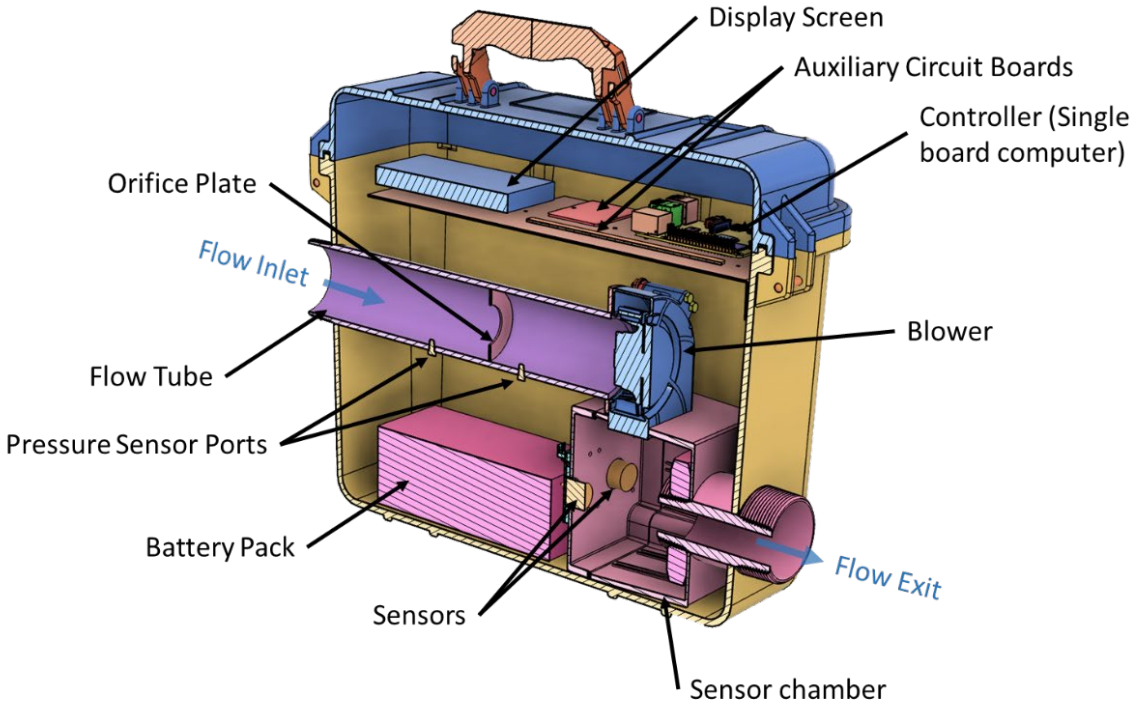

Figure 6: Cutaway schematic of the integrated instrument.

Principal mechanical components are shown in Figure 6. An overview of the instrument operation is provided here with details of key components in the next section.

Air flow path: In operation, the inlet is equipped with a hose-attachment fitting that rapidly connects to a hose. Multiple hose types can be used; the OS-HFS utilized the hose provided with CSU's BHFS instrument. The selection of the length and type of hose influences the maximum flow rate through the instrument. In general, shorter hoses have less flow resistance, leading to

higher air flow rate through the instrument, which is important to measure larger emissions. An inlet screen is also required, either as part of the hose attachment or at the inlet to the instrument.

The blower draws in the emissions through the flow tube and orifice plate, and discharges into the sensor chamber. By placing the sensors directly in the flow path, no sample pumps are required to extract part of the flow stream for measurement, reducing the complexity of the instrument.

The flow is directed out the flow exit. In operation, this port is equipped with a screen to keep foreign matter from the sensor chamber. In some cases, it may be useful to attach a discharge hose to direct the captured emissions away from the instrument and operator. This can be accomplished using the same fittings and hose type as the inlet. Increased flow resistance caused by the discharge hose will reduce the maximum flow rate through the instrument and the maximum emission rate that can be measured.

Sensing: Total flow is measured by pressure drop across the orifice plate in the flow tube, using a differential pressure sensor. The flow tube dimensions provide sufficient stability for the orifice plate to measure the flow rate. Changes in these dimensions should be analyzed thoroughly. The size of the flow tube and blower practically set the horizontal dimension of the instrument, and all other components are positioned relative to the volumes of those components.

The sensor chamber includes mounts for gas sensors. The prototype instrument used two sensors. More/fewer sensors could be installed in the same chamber with some re-engineering. Pressure fluctuations from turbulent air flow at the blower exit may affect sensor readings. Some sensors may need to be sheltered or placed in separate sensor chambers supplied by sample pumps. Many gas sensors also report temperature, pressure, and relative humidity which may be useful for advanced calibration corrections and for translating measurements to standard conditions.

As a general rule, the architecture favors the use of sensors with digital outputs. This approach eases the integration with other instrument electronics (see next section), and the integrated amplification, A/D conversion, and correction reduces sensor noise issues presented by using separate Wheatstone bridges and A/D conversion. It does, however, limit the choice of sensors and the speed at which the sensor can be read. In practice, these limitations did not unduly restrict the design of the system and are highly recommended for derivative devices.

Electronics: Electronics include an SBC that provides supervisory control, user interface, and data management for the instrument, and auxiliary electronic boards that integrate necessary components for integrating sensors and battery management.

Enclosure: The enclosure uses a commercially available, water- and dust-tight, case. All components are inserted into the enclosure from the top of the unit. This restricts access to the components but maintains the integrity of the enclosure.

The main battery, which powers the fan and several other components, is located on the bottom of the enclosure to keep the center of gravity low, helping stabilize the unit when stationary or carried. The SBC utilizes a separate battery and will continue to function when the main battery is discharged. Charging of the main battery occurs *in situ,* without removing it from the case, using appropriate connections. The auxiliary SBC battery charges from the main battery. In the prototype, charging is done with pigtails inside the box, while a productized unit would likely have bulkhead connectors installed in the case.

The airflow path is sealed, and sealed to the case, to minimize gas intrusion into the electronics area. A complete seal is, however, impractical. Evaluation of possible gas intrusion and ignition sources are part of the safety review required for any completed instrument.

3.1.2 Electronics Architecture

This section discusses the design and interconnections of electronics components. See PCB files in the data archive for details.

A primary goal of the electro-mechanical architecture was to allow easy replacement (or substitution) of sensors and controls. The architecture utilizes an industry-standard SBC (Raspberry Pi™) and the Python programming language. This class of computer is inexpensive, powerful, relatively low power, and integrates well with other computational systems, including networking and Bluetooth devices. The programming language is transportable to other, similar computer platforms, and the I/O ports of any similar SBC can be readily mapped to talk with the sensor systems via common serial port standards. Finally, this class of computer supports quality display screens, with backlights, that enable a modern user interface and make diagnostics, data upload, and field operation easier than the 4-line LCD display utilized in the BHFS.

Additionally, the move away from proprietary controllers supports fast upgrading of the instrument's supervisory control components; SBCs evolve rapidly over the life of an instrument and building around a proprietary microcontroller may retard adaption of the instrument to evolving use patterns. The inability to upgrade the existing BHFS instrument makes time-series data collection difficult, prevents effective measurement automation, and effectively prevents the integration of new or different sensors.

As a key example of integration, many companies are moving toward integrated data tracking systems for their leak detection and repair (LDAR) programs. Automated integration of leak measurement to these tracking systems would reduce data errors, provide better tracking of detection and measurement, and reduce regulatory reporting burden. A complete redesign would be required to adapt a BHFS to this type of communication. In contrast, the OS-HFS' SBC controller could be readily adapted to upload leak measurements to a server, using standard data interchange protocols.

Figure 7 provides an overview of the electronics and sensing architecture of the OS-HFS.

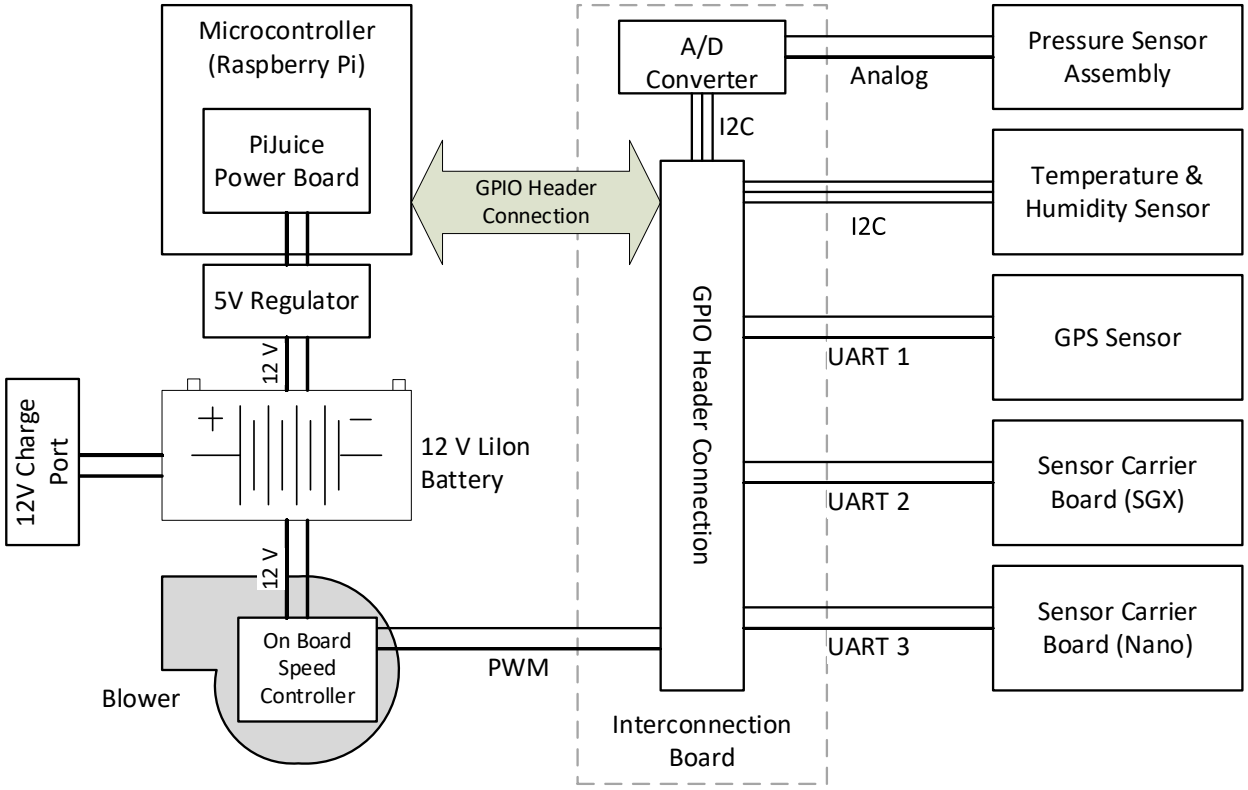

Figure 7: Electronics architecture for the prototype unit.

Overview: Primary control is accomplished by an SBC. A Raspberry Pi was selected for the prototype, as it has sufficient general-purpose (GPIO) pins and runs a robust version of the Linux operating system. The SBC also drives the display screen, using an HDMI standard driver with a touch screen add-on.

A GPIO header connector expands the GPIO pins for access to multiple other components. In general, each of these is on a separate board, and dispersed throughout the instrument to suitable locations for sensing or control. The GPIO break-out is a commercial product (Raspberry Pi Cobbler from Adafruit[*]). In a production unit, the breakout would be mounted on an instrument-specific PCB that would then fan out connections for other subsystems. For the OS-HFS, a plug-board was utilized, as shown in Figure 8. In the prototype, there is no cover over the electronics assemblies; a production unit would have a sheet metal or conductive plastic cover.

PCBs: Both sensors utilize a 5-pin mounting that required a custom PCB to securely hold the sensor and mount it in the sensor chamber. Both sensors performed A/D conversion, calibration corrections, and noise reduction internal to the sensors, and communicated results via a serial connection (see Figure 7 for the types of serial connection used). Therefore, the PCB provided only serial and power connections; no other active components were required. The PCB must also be

[*] https://www.adafruit.com/product/914

designed to mount securely to the sensor chamber and provide space for a gas-tight seal around the sensor.

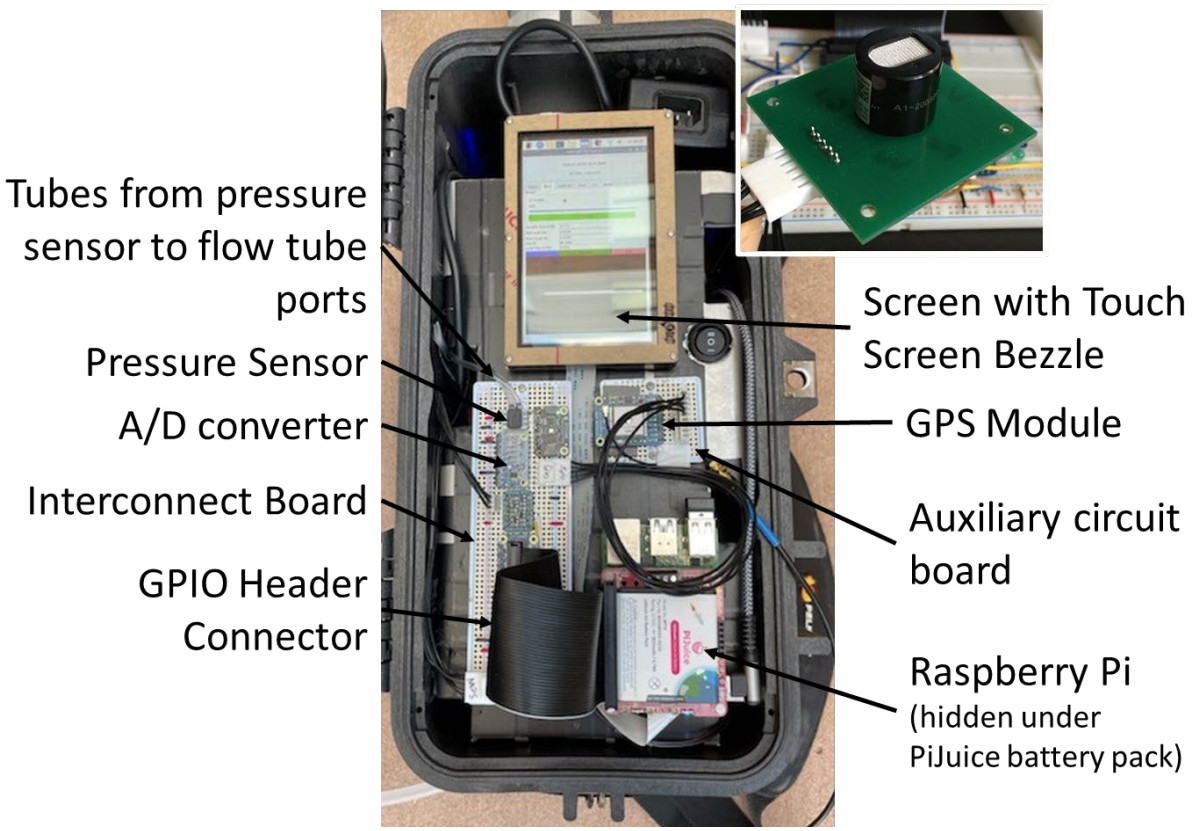

Figure 8: Photos of key electronics assemblies. Main photo shows the top of the prototype with key electronics assemblies visible. Inset photo shows the mounting PCB for the sensor elements.

Blower speed control was accomplished by sending a pulse width modulation (PWM) signal to the blower's on-board controller. This method simplifies electronics complexity, as no H-bridge or similar motor drive is required, and provides better noise suppression, as all switching occurs close to the fan. It is highly recommended that any production units identify fans with internal speed control functionality.

The interconnection board primarily mapped incoming serial ports, or the outgoing PWM signal for the blower to the GPIO ports on the controller, although some level shifting from the Raspberry Pi's 3.3 V to 5 V was implemented for some interface functions. GPIO mapping was accomplished in software.

Data communications: With the exception of the pressure sensor, all sensors were selected to communicate over serial ports. There are two advantages to this strategy. First, sensors with integrated A/D conversion, scaling, and calibration tend to be more stable and less susceptible to electrical noise in the instrument. Since these critical functions are inside the sensor module, this also supports fast replacement of any failed assemblies. Second, sensors can be positioned as needed within

the instrument, and do not need to be located on the main PCB. This eliminates supporting equipment, such as sample pumps for gas sensors, and reduces the amount of electrical shielding required, although shielded connection wire is recommended.

The pressure sensor (Honeywell HSCDRRN002NDAA5) used a commercially available A/D converter board (Adafruit carrier board* for the TI™ ADS1115 I2C A/D converter chip) to perform A/D conversion and communicate results back to the SBC using serial (I2C†) communications. I2C versions of this pressure sensor are available but were out of stock during prototype development. Since any differential pressure sensor will require tubing from the pressure ports in the flow tube to the pressure sensor, the sensor unit can be located on the same circuit board as the GPIO breakout.

The GPS module provides both time and location to the SBC. Since data files are often processed using time stamps to combine multiple data streams, accurate timing is essential. The GPS module uses an auxiliary antenna mounted within the plastic instrument enclosure. If a metallic enclosure type is utilized in derivative units, some provision for an external antenna may be required. GPS may also be required to integrate the location of measurements into companies' data tracking systems.

Communication speeds vary between sensors (see Section 3.2 for key sensors), but since none of the sensors needs to be sampled at more than a few Hz, serial communications are sufficiently fast to simultaneously read all sensors.

Power management: All power was provided to the prototype using the 12 V lithium-ion battery. The battery was purchased with a charger. The blower is connected directly to the battery, and the instrument will not function without sufficient charge in the main battery. The SBC was powered from an onboard lithium-polymer battery (a PiJuice™ battery pack‡) via a 12 to 5 V regulator. The operational plan for the power system is:

1) Operator charges the main 12 V battery in the unit overnight and possibly during breaks, such as when driving from facility to facility.

2) The PiJuice pack is charged from the main battery and requires no direct attention from the user.

* https://www.adafruit.com/product/1085?gclid=Cj0KCQiAmKiQBhClARIsAKtSj-mfjMTuiiBfQe9myI45V6enMEQ9GxW7dEGcl1MfewyX5R6_fjnoFu0aAqAXEALw_wcB

† I2C or I^2C is a commonly utilized serial communications protocol that can accommodate multiple slave components on one serial connection. See, for example, https://en.wikipedia.org/wiki/I%C2%B2C

‡ https://uk.pi-supply.com/products/pijuice-standard?_pos=21&_sid=4a1f56936&_ss=r

3) The SBC remains powered when the main battery is disconnected or discharged, for 1-3 hours, allowing data upload and other maintenance operations. This also prevents loss of settings, etc. if the main battery runs low during use.

3.1.3 Software Architecture

The software running the OS-HFS is written in Python, a platform-independent interpreted language. GUI elements are currently implemented using PyQt5, but the modular software approach allows for easy substitution of other GUI libraries. The software architecture closely resembles the hardware architecture as it is implemented using an object-oriented approach (see Figure 9). "Reader" classes communicate directly with each sensor or peripheral device based on manufacturers' datasheets and any undocumented behaviors observed during testing. Each reader class maps appropriate lower-level commands and responses specific to each sensor into a common command/response queue for use in other instrument functions. A "Hi Flow" class orchestrates the critical functions of the OS-HFS by issuing commands, receiving responses, performing calculations, and updating the GUI. This class also handles file I/O and measurement data storage. The current prototype software has been supplied to CARB and is identified in Appendix A.

Since the OS-HFS is implemented on an SBC with a full Linux operating system rather than a microcontroller, display and device interfacing is streamlined, and networking capabilities are intrinsic to the SBC's operating system, including Wi-Fi, Ethernet, and Bluetooth. The current implementation is built as a desktop application, but the SBC could easily serve the application on a web interface where it would be available to any mobile device with Wi-Fi and a web browser.

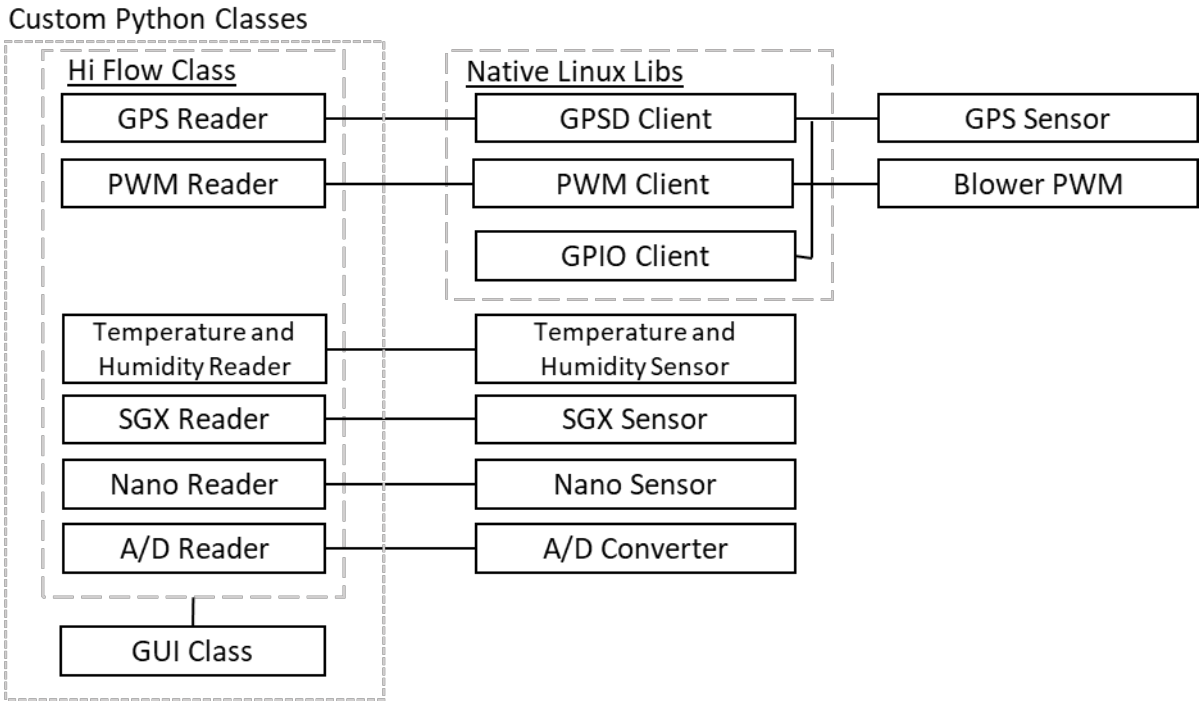

Figure 9: Software architecture schematic. Custom Python classes interact with native libraries or with physical sensors directly. The software architecture follows the modular approach of the physical architecture.

The prototype improves the user experience by providing detailed information to the user on a color touch screen display. From the display, the user can view all instrument parameters, calibrate sensors, and perform system checks. The user can also save instrument data electronically using an automated measurement cycle or start and stop a "manual" measurement that captures time series data without intervention from the instrument. At the end of each measurement, leak rates and summary data are provided along with data quality indicators. By using an SBC, data can be logged to standard file formats, and accessed using file transfer and connectivity with other devices. This also opens the possibility of real-time data transfer by pairing the OS-HFS with auxiliary devices over Wi-Fi or Bluetooth®.

A screenshot of the OS-HFS GUI is shown in Figure 10.

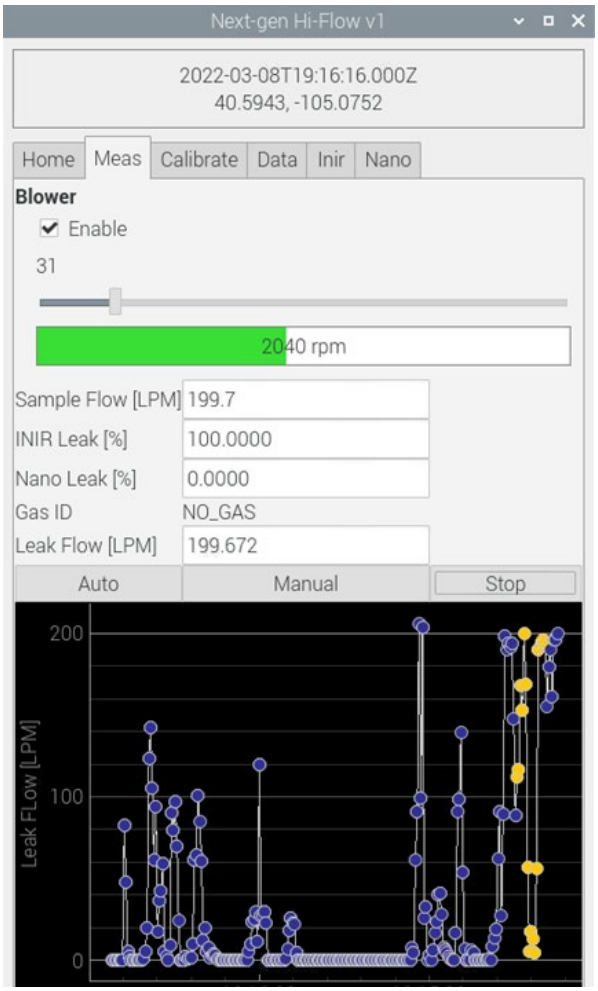

Figure 10: Example GUI tab as shown on heads-up display or a virtual desktop accessible by a Smartphone, table, or remote PC. The screenshot was taken during a debugging session, not during an actual measurement.

Time and location data are always shown in the header box at the top of the screen. This data is supplied directly by the GPS unit, and is thus always correct, with minimal offset from the true time. Several tabs provide access to the various functions needed to operate the device including direct access to the instrument's sensors (named the "INIR" and "Nano" throughout this report; see Section 3.2.3) to perform zero, span, and offset calibrations. General device parameters are displayed as well, and other command-based interactions are available.

The measurement tab ("Meas", Figure 10) is of most interest during measurement activities. Here, the operator can enable or disable the blower and change the setpoint of the blower. The current PWM setting along with blower speed in rpm are shown. The measured sample flow is also shown along with the concentration measured by each sensor, and the gas molecular weight classification provided by the Nano sensor. Finally, the leak flowrate is shown, and plotted on a time series graph. Stability of concentrations shown on this graph provides an invaluable tool for experienced HFS practitioners.

Auto, Manual, and Stop buttons are used to save data to a delimited text file that includes all available input parameters and the resultant calculations. The Auto button starts a timed measurement cycle that automatically stops and saves a measurement file when completed.

The Auto mode implements a typical fugitive measurement, and the timer is set to a two-minute-long measurement period by default. Future extensions to the software could automate more of the measurement process following the outline in section Appendix B including automatic flowrate adjustment. This type of implementation could potentially reduce training requirements for operators.

The Manual button allows the operator to run a longer measurement but requires the Stop button to be pressed to conclude the measurement. A default timeout can be set to intervene if a measurement is not stopped manually. This mode is intended for "long-term" measurements, for example, to estimate emissions from time varying sources. A representative sample time can be used at the operator's discretion up to the length of the battery life of the unit.

All leak flow data are shown on the time series graph. During an active measurement (either Auto or Manual) the data points are shown in yellow to differentiate them from idle points on the graph that were collected prior to the start of the measurement, and to indicate that a measurement is underway. In the version 1 prototype the INIR sensor was considered the main sensor and the estimated emission rate was calculated based on its output, as can be seen in Figure 10.

> **Note:** The project team made every attempt to utilize only open-source software libraries for the prototype unit. However, any party adopting the OS-HFS design should check all libraries utilized to ensure that their use is compatible with the licensing of the libraries.

3.2 Selection of Key Components

3.2.1 Blower

The user manual for the BHFS[19] states that the device can produce a maximum of ~10 SCFM (283 LPM) at initial flow with full battery. The measurable leak rate is listed as 0.05 to 8.0 SCFM (1.42 to 226 LPM), though the device will display readings down to 0.1 LPM when the display is in the LPM mode setting. Testing shows that while the BHFS display reports readings below the stated lower limit, the accuracy is questionable, and it may be that the stated 1.42 LPM lower limit is that which still meets the stated system accuracy (± 10 % by volume leak rate reading, methane). Preliminary calculations made using various blower and sensor combinations under consideration indicated that 0.1 SLPM was a reasonable target for a lower usable limit in the OS-HFS. Similarly, the target upper limit for the OS-HFS design was set at 12-15 SCFM (336-420 SLPM). This target would expand the BHFS capabilities by ~50 % while still allowing the prototype to be a more compact device.

The BHFS uses the 3M™ GVP-100 Motor Blower, to create the flow stream which draws the emission and excess air into the device. The GVP-100 is a component of a Powered Air Purifying Respirator system marketed by 3M that consists of the blower, a power cord, and a battery pack. The respirator system has been classified as intrinsically safe for use in hazardous locations. Performance curves for the GVP-100 blower did not appear to be readily available, so a test rig was created to develop a fan performance curve as the basis for identifying suitable replacements. A spare (non-working) BHFS unit was provided to the project in kind by Heath Consultants Inc. The blower was removed and tested by applying full power and gradually blocking the outlet and monitoring the static pressure produced as the flow rate decreased. This procedure is a simplified version of the formal test procedure used to characterize fans and blowers in industry[32]. The resulting fan curve is shown in Figure 11. Similar fan curves can be obtained from fan manufacturers; other units under consideration are shown in Figure 11, for comparison.

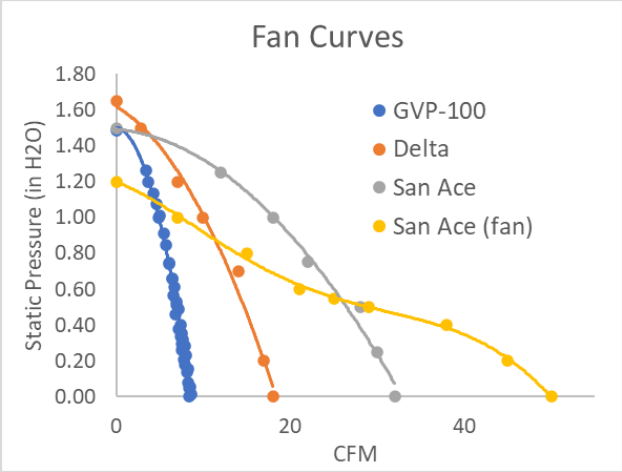

Figure 11: Fan curve comparison for the GVP-100 blower used in the BHFS vs. other models under consideration from San Ace and Delta Fan. The yellow trace (San Ace (fan)) shows the performance of an axial fan, for comparison. The performance curves for the GVP-100, Delta, and San Ace are typical of centrifugal blowers.

When selecting a fan for a given application, the fan should be chosen such that it is generally operated below the stall region (the region where, starting from maximum flow and following the curve, the curve begins to flatten). Thus, the desired flow rates should be available when the needed static pressure is at or below the stall region. In Figure 11, the curve for an axial fan (San Ace (fan)) is shown alongside performance curves for centrifugal blowers – two common fan designs used in electronics cooling applications. The shape of the GVP-100 curve indicates that it is likely a centrifugal blower, which was not obvious from observing the design of its housing. For a similar flowrate, package size, and power consumption, centrifugal blowers are generally able to produce a higher static pressure at a given flowrate compared to axial fans. Observing the yellow curve (San Ace (fan)) the axial fan shows a more drastic reduction in flow with increasing static pressure. Thus, centrifugal blowers should provide a more stable flow stream that is less sensitive to changes in back pressure. This characteristic may be advantageous during field measurements where a wide

variety of measurement situations will be encountered and will likely require a variety of attachments to collect the emissions.

Special consideration must be given to ensure that the blower will be safe for use in direct contact with gas/air mixtures that may be within flammability limits. This automatically points to brushless motors suitable or certified for use in hazardous locations (e.g., UL Class/Division, ATEX, HazLoc, IECEx, etc.). To better understand the characteristics of an intrinsically safe blower, first the GVP-100 from the spare BHFS was disassembled to study its construction. As shown in Figure 12, the blower was constructed primarily of plastic with a metal shaft and small electric motor. All the electrical connections directly in contact with the flow stream were potted (encased) in epoxy, and the inside surfaces in contact with the flow stream were sealed from the outside. The blower was a centrifugal design, in line with results of the fan curve testing.

A search for DC centrifugal blowers certified for use in hazardous locations did not identify any units available commercially off the shelf. Conversations with several manufacturers revealed one company willing to make them on contract with a specified minimum order and production period, along with fees for engineering services and certification. Two other manufacturers who recently started producing ATEX rated fans were also identified. Both manufacturers were producing axial fans for use with AC mains power. When asked about the availability of DC centrifugal blowers with ATEX certification, both manufacturers stated that the intended application for the ATEX axial fans was in new commercial refrigeration units that use hydrocarbons as the working fluid. They stated that a DC centrifugal blower that was certified was not likely to be produced unless there was a similar new, widespread market demand.

Figure 12: Inside the 3M GVP-100 blower motor used in the BHFS. The blower is certified for use in hazardous areas. All the internal electrical connections are encapsulated. The internal housing (upper left) is characteristic of a centrifugal blower design.

The ATEX rated axial fans from both manufacturers had similar part numbers designating non-ATEX units with otherwise identical specifications. The non-ATEX units were IP68 rated against water and dust ingress and featured encapsulated electrical connections and non-sparking materials, much like the GVP-100. To compare rated and non-rated units, one of each model of fan was acquired and disassembled for study, revealing little, if any, difference between the two units. The only difference observed was so minor, that it may be attributable to manufacturing variance. The manufacturer declined to comment on this matter.

Based upon this result, the project team made two assumptions. First, the DC units were likely not ATEX certified due to lack of demand, and second, the required engineering to make an ATEX-

compliant unit was likely small. The team chose the San Ace 97W, an IP68 rated, DC powered centrifugal blower for use in the prototype. Production units or subsequent prototypes may require the use of other blowers or contracting with the manufacturer to develop the correct certifications.

Two units were acquired, and one was disassembled for study. The project team found encapsulated electrical connections and components, with components made of aluminum, stainless steel, brass, and plastic. However, the housing was not gas tight and had vents or drain holes in the housing. For use in the prototype, these were sealed with silicon adhesive to completely contain the flow stream within the housing.

3.2.2 Flow Measurement

An orifice plate flowmeter is a standardized, well-documented flow measurement technique with a simple design and low component count that is relatively easy to implement. An orifice plate flowmeter works by measuring the pressure drop caused by the increase in flow velocity in the presence of a sharp-edged flow restriction within a closed pipe. Several documents describe the design considerations and uncertainties associated with orifice plate meters, including AGA Report 3.1[33] and ISO Document 5167[34]. An orifice meter was also used in the BHFS. Flowrate measurements reported by the BHFS were compared to a recently calibrated laminar flow element over a range of flowrates between 100 and 250 LPM and found to agree within 5 %, as specified in the BHFS manual. Given the performance of the BHFS flow measurement and the ease of implementation, an orifice plate meter was selected for use in the OS-HFS.

The flowrate and associated uncertainty reported by an orifice plate flowmeter constructed and implemented according to the ISO and AGA standards should be well-characterized; measurements made without additional calibration should fall within the specified tolerances, by design. Often, a meter calibration is used to account for any unavoidable deviations and to characterize a specific meter, in situ. The resulting “meter factor” characterizes the deviations of the meter under calibration relative to flow through a reference instrument. The meter factor is then applied to the in-use readings to align them with the reference standard. The OS-HFS uses this type of independent calibration and correction.

The ISO 5167 standard offers detailed guidance on the construction of an orifice plate flowmeter. However, the guide does not cover orifice plates for use in pipes less than 50 mm in diameter or at Reynolds numbers less than 5000. Reynolds numbers calculated for OS-HFS target flow rates generally exceeded 5000 in a 2 in diameter pipe, making this a suitable starting point for the design. The 2 in pipe also supported the desired increased flowrate relative to the BHFS, while supporting a similar or smaller package with similar power requirements.

The practical accuracy achievable with an orifice plate constructed in accordance with the standards will be limited by the accuracy of the differential pressure measurement, and any environmental factors present that influence that accuracy[33]. The accuracy can also be limited by the uncertainty in the discharge coefficient, which is determined experimentally or from empirical

equations based on large numbers of experiments. The ratio of the uncertainty in the empirical discharge coefficient (C_d) at a given Reynolds number (Re) to the uncertainty in C_d at an infinite Re is minimized when the diameter ratio β is ~0.56; these dimensions were utilized for the OS-HFS.

During the fan flow curve testing for the GVP-100 it was observed that the maximum static pressure produced was ~1.5 in H_2O. The original BHFS was equipped with a differential pressure (ΔP) sensor with a ~15 in H_20 range (MPX5004DP). The fan curves published by the blower manufacturers showed a maximum static pressure of 1.5 in H_2O at zero flow. This meant that the full range of the sensor used in the BHFS would not be needed in practice, and that the resolution of the instrument could be improved by substituting a sensor with a reduced range. The OS-HFS uses a sensor with a range of ±2 in H_2O to improve resolution, which covers expected pressure differentials but protects the sensor from over pressure in the event of a complete exhaust blockage. The chosen sensor has an accuracy of ± 0.25 % (versus ± 1.5 % for the BHFS' sensor). The combination of restricted range and better accuracy improves the resolution and the overall accuracy of OS-HFS' flow measurement relative to that of the BHFS.

OS-HFS flow measurement was calibrated using tracer gas dilution in accordance with ASTM designation E2029-11[35]. CP grade methane (Airgas, Inc.) was metered at a constant flow of 13 SLPM* through a critical orifice and introduced at the inlet of the OS-HFS sample hose. Upstream pressure and temperature were monitored for consistency, and the downstream flow was verified with a volumetric prover (Bios DryCal) reporting in standard units. A methane analyzer (QC-TLDS, Aerodyne Research Inc.) measured the methane at the exit of the OS-HFS by drawing a sample from an inlet placed in the center of the OS-HFS sensor chamber. The methane analyzer measurement range is 0-200 ppm methane with a 1-second precision of 0.3 ppb. During testing, the PWM controller of the OS-HFS fan was used to vary the setpoint between 20 % and 100 % duty. The methane tracer gas flowrate was held constant. methane readings ranged between 30 and 60 ppm during testing; background methane concentrations (in ambient air) were taken between each PWM setpoint to calculate the enhancement due to tracer gas flow.

This calibration procedure was performed twice. Both tests were performed in Fort Collins, CO at an elevation 5,003 ft above sea level at a station pressure of ~12.2 psia. The first test was performed on 7/9/2021, at an ambient temperature of 27 °C using a 2 in diameter antistatic vacuum hose on the OS-HFS inlet. Results are compared in Figure 13, first for a constant C_d based on the empirical formulation found in the standards, and second with a meter-specific C_d developed as a function of ΔP – i.e., by solving for the unknown C_d at each test point. For the parameters of the OS-HFS design, the empirical C_d was 0.637, while the meter specific C_d varies between 0.674 and 0.656 for Re ranging from $6.8x10^3$ to $12.6\ x10^3$. The maximum ΔP achieved during testing was 0.72 in

* Standard conditions are 25 °C / 1 atmosphere throughout.

H_2O. In this configuration the OS-HFS was able to achieve a maximum flowrate of 442 SLPM, which was well aligned with the target design goal.

In subsequent testing, the antistatic vacuum hose used during the first test proved too stiff for practical use when tested at CSU's METEC facility. Therefore, the OS-HFS was modified to use the hose from the BHFS. A second calibration was conducted using the BHFS hose on 12/19/2021 with an average ambient temperature of 19 °C. In this configuration the OS-HFS was able to achieve a maximum flowrate of 316 SLPM, as shown in Figure 13. In this configuration the C_d varied from 0.677 and 0.651 for Re ranging from $4.6x10^3$ to $9.8x10^3$. The maximum ΔP developed was 0.36 in H_2O. As can be seen in both Figure 13 and Figure 14, the empirical discharge coefficient differs from those obtained specifically for the OS-HFS by direct calibration. In both cases C_d varied with flow (and thus ΔP) and results were improved by applying C_d as a function of ΔP. In each case a single C_d of 0.667 would likely be suitable over the flow ranges tested and would not degrade the accuracy greatly.

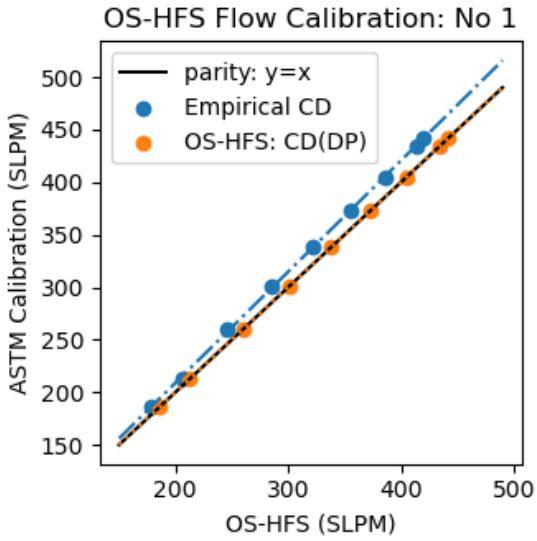

Figure 13: First OS-HFS flow meter calibration performed in July 2021 using a 2 in diameter antistatic vacuum hose.

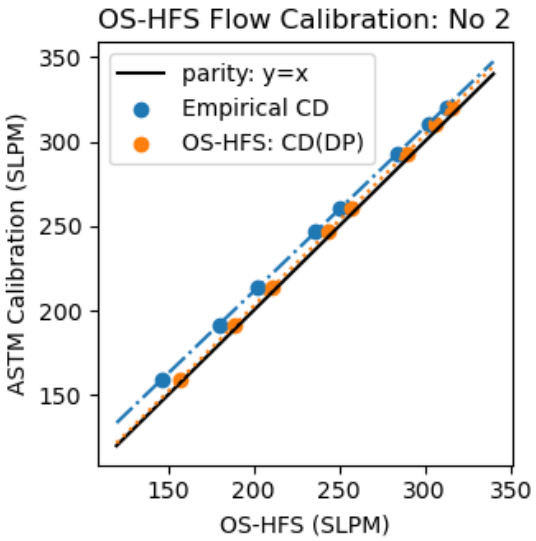

Figure 14: Second OS-HFS flow meter calibration performed on 12/19/2021 using the inlet hose from the BHFS.

3.2.3 Concentration Measurement

The BHFS used a pellistor-based sensor (e.g., SGX Sensortech VQ549ZD series) which was operated in both catalytic oxidation and thermal conductivity modes. The sensor is not methane-specific, and its output varies with gas composition. The catalytic nature of the sensor makes it vulnerable to both saturation and poisoning by other gas species that may be encountered in field use (e.g., higher hydrocarbons, oil mist, H_2S, etc.).

The precise implementation of the sensor within the BHFS is a trade secret, but many have observed a "transition behavior" around the 5 % concentration, which is generally assumed to be the

transition between catalytic oxidation mode and thermal conductivity mode, or the transition between calibration curves. This transition may be noted by observing the number of digits displayed on the BHFS screen; no other indication is displayed.

The goal of selecting sensors for the OS-HFS was to (a) alleviate identified sensor issues, (b) modernize communication between the SBC and sensors, (c) mitigate other use issues while still selecting readily available, moderate cost, sensors. A market survey indicated that component-type sensors and modules targeted at industrial applications met these requirements, as shown in Figure 15.

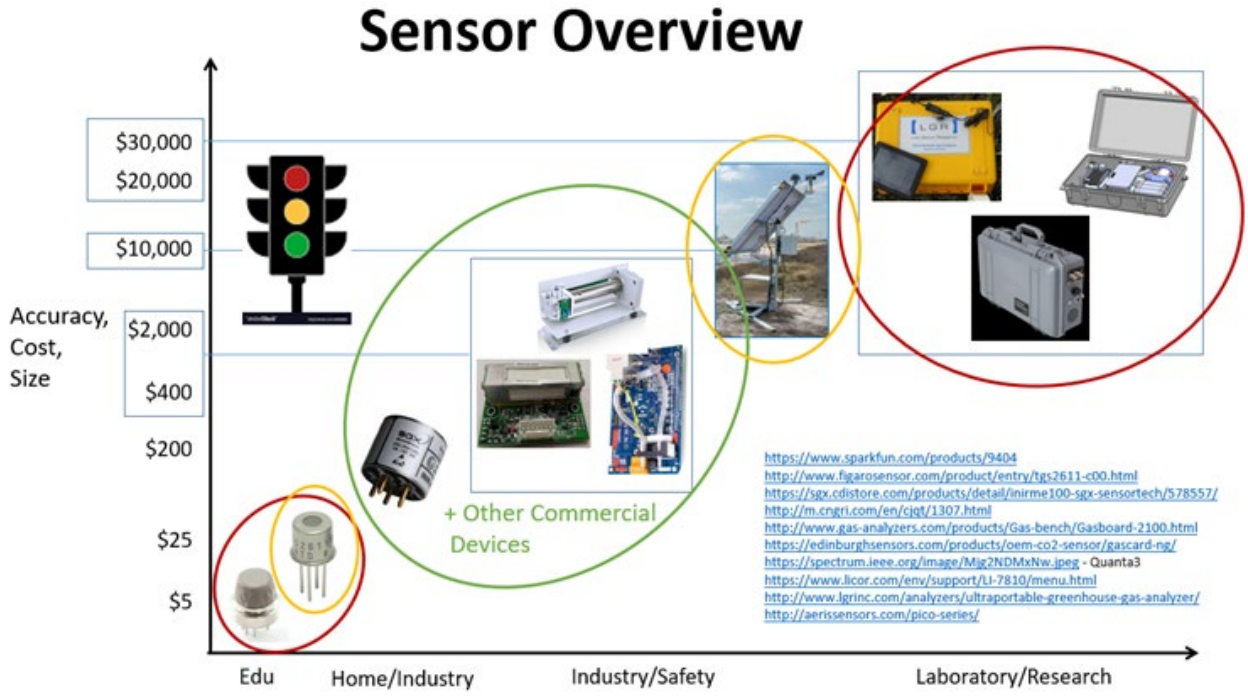

Figure 15: Sensor selection strategy for OS-HFS development. Avoid low-cost sensors with poor accuracy, and avoid high-cost sensors with great accuracy, but increased size. Focus on compact, readily available industrial sensors with reasonable accuracy and affordability.

Two sensors stood out based on manufacturer specifications, availability, and cost (Figure 16):

1. *SGX INIR-ME100*[*], a non-dispersive infrared (NDIR) sensor. Key datasheet claims include a "Triple Range" (0-1 %v, 1-4 %v, >4 %v) operation, a resolution of up to 10 ppm, and an LDL of 100 ppm.

2. *Nevado Nano MPS flammable gas sensor*[†], which the manufacture calls a "molecular property spectrometer" with some ability to differentiate between gas species (or mixtures) based on average molecular weight. Key datasheet claims include a methane detection

[*] https://sgx.cdistore.com/products/detail/inirme100-sgx-sensortech/578557/
[†] https://nevadanano.com/mps-flammable-gas-sensor/

range of 0-100 % LEL, a resolution of 0.1 % LEL, an accuracy of ± 3 % of LEL from 0-50 % LEL. In operation the sensor could also report by % volume (as opposed to % LEL) and was used in that mode in the OS-HFS.

Both sensors are integrated packages with onboard diagnostics and control, requiring only power and communication connections. The initial design intent was to use the wider range and higher resolution of the INIR sensor as the primary sensor, and the Nano as a secondary sensor to provide corrections or additional calibrations based on the type of gas being measured. For example, the Nano can distinguish between 6 classes of gases or gas mixtures. This would enable switching between a family of built-in calibrations for the INIR sensor to improve the accuracy of measurements made at various locations in the natural gas supply chain with varying compositions.

Figure 16: The SGX INIR-ME100 and Nevada Nano MPS Flammable Gas Sensor were chosen for use in the prototype OS-HFS.

To understand the behavior and performance of the sensors, a sensor test rig was developed to hold 2 each of INIR and Nano sensors as shown Figure 17. At the time of testing, it was discovered that the INIR sensors were using different firmware versions (2.25 and 2.33); users of the OS-HFS design may wish to control this variable, as the performance and interfacing may differ between firmware revisions. Testing characterized each sensor's performance over a range of gas concentrations and varying atmospheric pressures. The INIR was found to have a consistent, non-negligible pressure dependency, as indicated in the datasheet. The Nano was found to exhibit much lower variation with pressure.

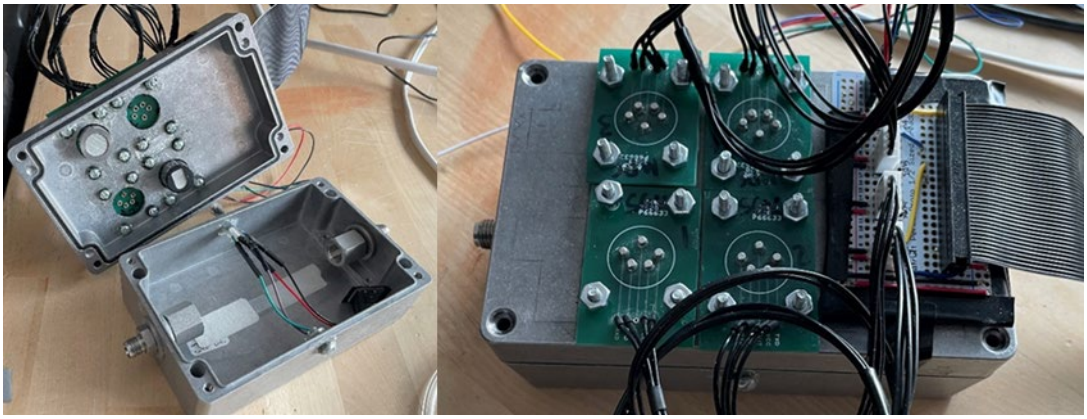

Figure 17: Test chamber for prototype sensor calibration and characterization.

During testing, methane/air mixtures were generated using choked flow orifices (O'Keefe) and calibrated volumetric provers (Bios DryCal). Gas mixtures were introduced into the sample chamber between 0.5 and 1 SLPM. A back pressure regulator was used to monitor the pressure within the chamber. Pressures were varied between 85 kPa and 100 kPa for each gas concentration blend introduced. Tests were performed with nominal concentrations of 200, 500, 1000, 2500 and 5000 ppm, 1, 1.5, 2, 3, 5, 10, 15, 20, 25, 35, 50, 60 and 80 % methane by volume in "shop-air" which had been filtered and dried by typical coalescing and particulate filters.

Prior to each test the INIR was zeroed and spanned according to the manufacturer's guidelines, with the chamber held at 90 kPa. The Nano does not require user calibration and is factory calibrated for five years. During testing it was observed that the Nano appears to "self-zero" during power up, and the presence of gas or ambient pressure can affect the output depending on the conditions present at power on. As a result, care must be taken to present only background air concentrations to the sensor at power-up.

An example time series from one of these tests is shown in Figure 18.

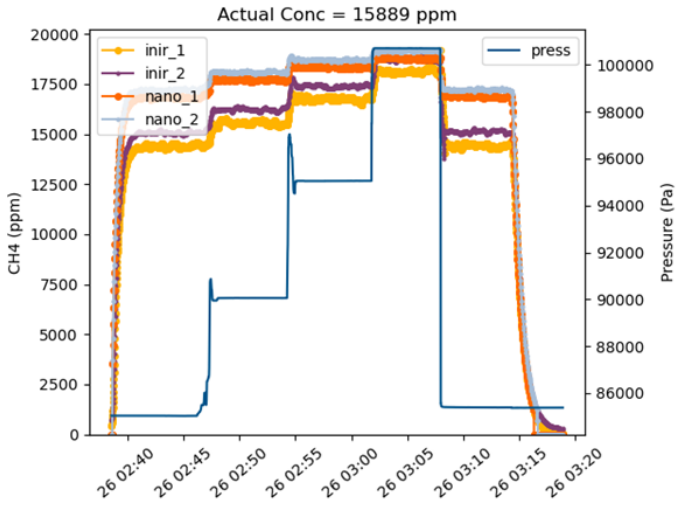

Figure 18: Example data capture from sensor characterization. The INIR sensor output varies with ambient pressure to a greater degree than the Nano sensor.

Briefly, a methane-air mixture at 1.5 % by volume was introduced into the sample chamber at 85 kPa until the sensor readings stabilized. Once stabilized, data were recorded for 5 minutes. Next, the pressure was changed to 90 kPa and the readings were allowed to stabilize before recording again. This procedure was repeated at 95, 100, and again at 85 kPa for a variety of gas concentrations. This testing took place over the course of several days during February and March of 2021.

It is evident from the testing that the INIR response is linear over the range of concentrations tested, and that there is a strong dependence on pressure, as shown in Figure 19. The readings are consistent at the calibration pressure of 90 kPa, 10 % low at 85 kPa, and 10 % high at 95 kPa. Therefore, the INIR sensor requires a calibration and correction for the prevailing atmospheric pressure. The INIR sensor was tested both with and without an offset calibration point. As the manual states, this step does not appear to be needed with the current firmware and does not seem to offer a significant improvement in performance.

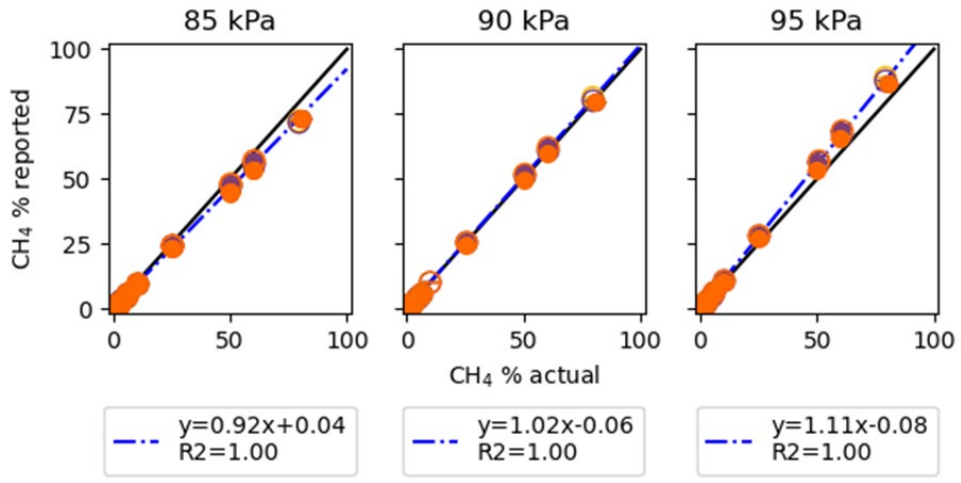

Figure 19: The INIR sensor shows a strong dependence on ambient pressure. A 5 kPa change from the 90 kPa baseline used for calibration results in a 10 % change over the tested range.

The Nano response to changes in pressure is less pronounced than the INIR, reading 1% lower than the 90 kPa baseline at 85 kPa, and 2 % higher at 95 kPa. The Nano under-reports the concentration present considering the full-scale results, as shown in Figure 20. It was also noted that the Nano reports 0 % concentration when the actual concentration falls below 1500 ppm and reports readings when the actual concentration is above 1500 ppm.

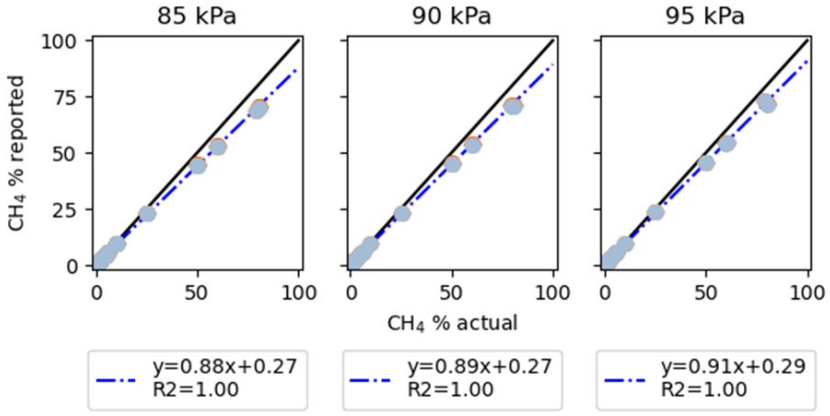

Figure 20: The Nano sensor output shows less pressure dependence but seems to consistently underestimate the gas concentration.

3.2.4 Background Concentration Measurement

The use of a background sensor is intended to account for any elevated gas concentrations in the ambient dilution air drawn into the HFS instrument along with the leak source being measured. Typically, the background gas concentration is subtracted from the measured gas concentration within the instrument to remove its contribution to the reported emission rate. This situation may occur, for example, on a small leak within an enclosed building with poor ventilation. If the

operator fully captures the leak source, the contaminated air being drawn in along with it will induce an additional sensor response, artificially inflating the reported measurement. A background sensor on the instrument could subtract the background contribution and report the true emission rate from the captured leak. This example assumes that the background sensor is measuring a truly elevated background, and not a parcel of air containing remnants of the emission source, other nearby emission sources, or the exhaust from the HFS itself. More typically, an incomplete capture is picked up by the background sensor, further lowering the reported emission rate from the source.

A background sensor located near the sample inlet could be useful as an indicator of incomplete capture but would be difficult include properly within the measurement strategy in all possible scenarios. For this reason and the fact that HFS quantifications are normally coupled with a primary means of detection, such as a handheld sensor or OGI camera, the project team decided to eliminate this feature from the prototype OS-HFS.

3.3 Accuracy Analysis

Once the prototype OS-HFS was assembled, several rounds of testing were conducted to quantify its performance and identify improvements needed. Tests were aimed at quantifying the lower detection limit, evaluating overall quantification accuracy, determining effects of varying gas compositions, and conducting practical use testing on "real equipment" at CSU's METEC facility. For each of the tests, readings from each of the two onboard sensors (INIR and Nano) were used to calculate results independently rather than using the Nano as an auxiliary sensor as originally planned, although use of the Nano as an auxiliary gas-type sensor could be useful with further development. Several follow up tests were performed in an attempt to identify the biases observed in the initial testing.

Testing methods are described in more detail in Section 4.

3.3.1 Lower Detection Limit

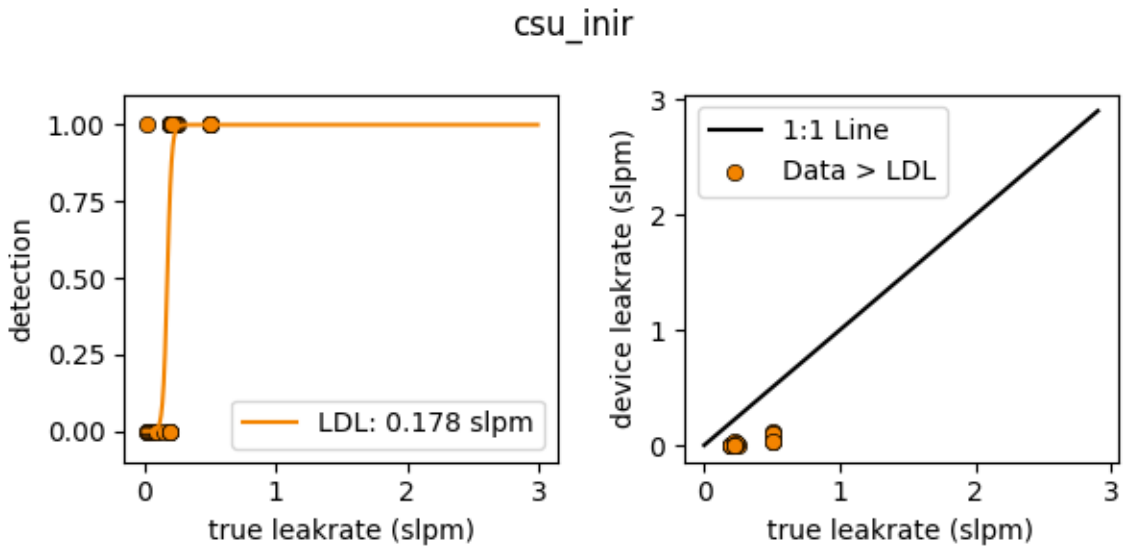

Figure 21: Prototype OS-HFS INIR sensor lower detection limit.

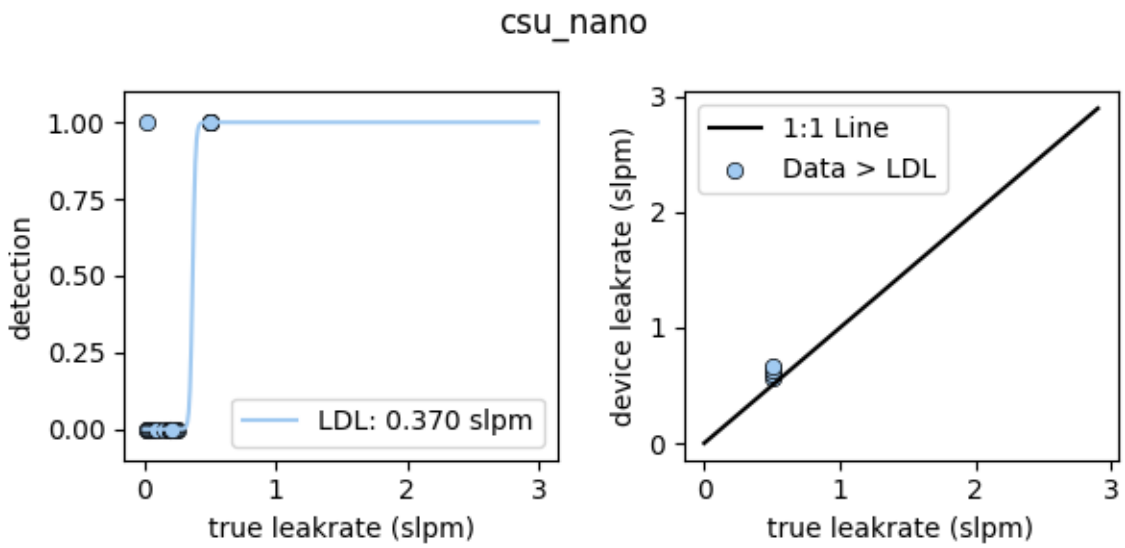

Figure 22: Prototype OS-HFS Nano sensor lower detection limit.

Lower detection limits (LDLs) were tested with the OS-HFS sample flow set at ~150 SLPM. Several data points were tested near the expected LDL and a logistic regression was performed on detect vs non-detect of the source emission. It should be noted that LDL as reported here only indicates the lowest test gas flowrate at which the HFS reported a non-zero emission rate and says nothing about the accuracy of the reported value. Based on the sensor data sheets, the INIR has a stated LDL of 100 ppm, roughly equivalent to an LDL of 0.015 SLPM. However, during testing these sensors did not detect concentrations with meaningful accuracy much below 1,000 ppm,

leading to an expected LDL of 0.15 SLPM. The LDL observed in system testing was close to this figure: 0.178 SLPM. The Nano sensor's datasheet states a detection range of 0-100 % of LEL (5 % vol/vol for methane) with an accuracy of ± 3 % of LEL. Interestingly, during testing it was observed that the Nano sensor would report 0 once the test concentration fell below 1,500 ppm and would resume reporting values once the test concentration was above 1,500 ppm. This would lead to an expected LDL of 0.225 SLPM, and the observed LDL was somewhat higher at 0.370 SLPM.

3.3.2 Quantification Accuracy

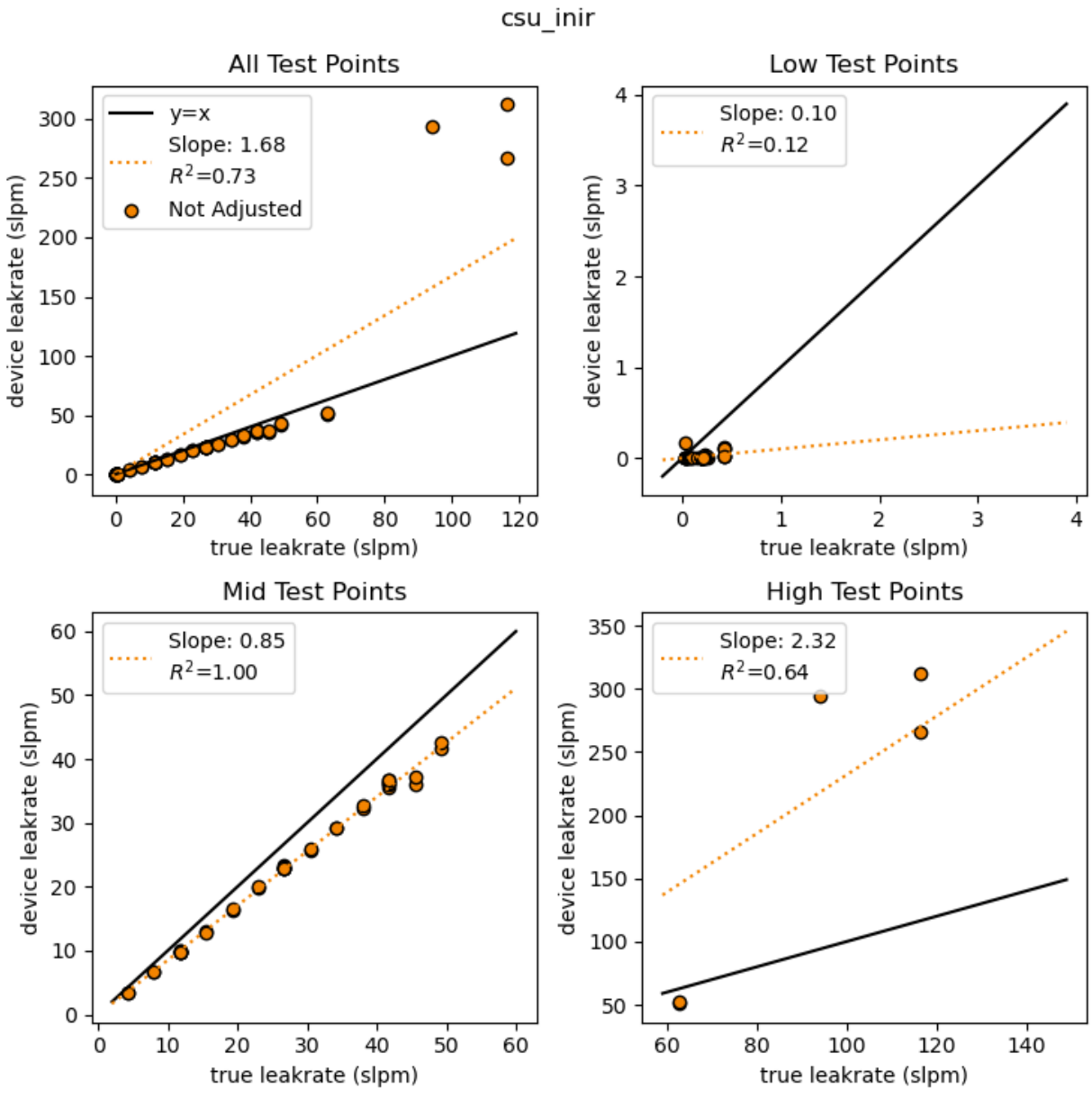

Figure 23: Prototype OS-HFS INIR sensor quantification accuracy.

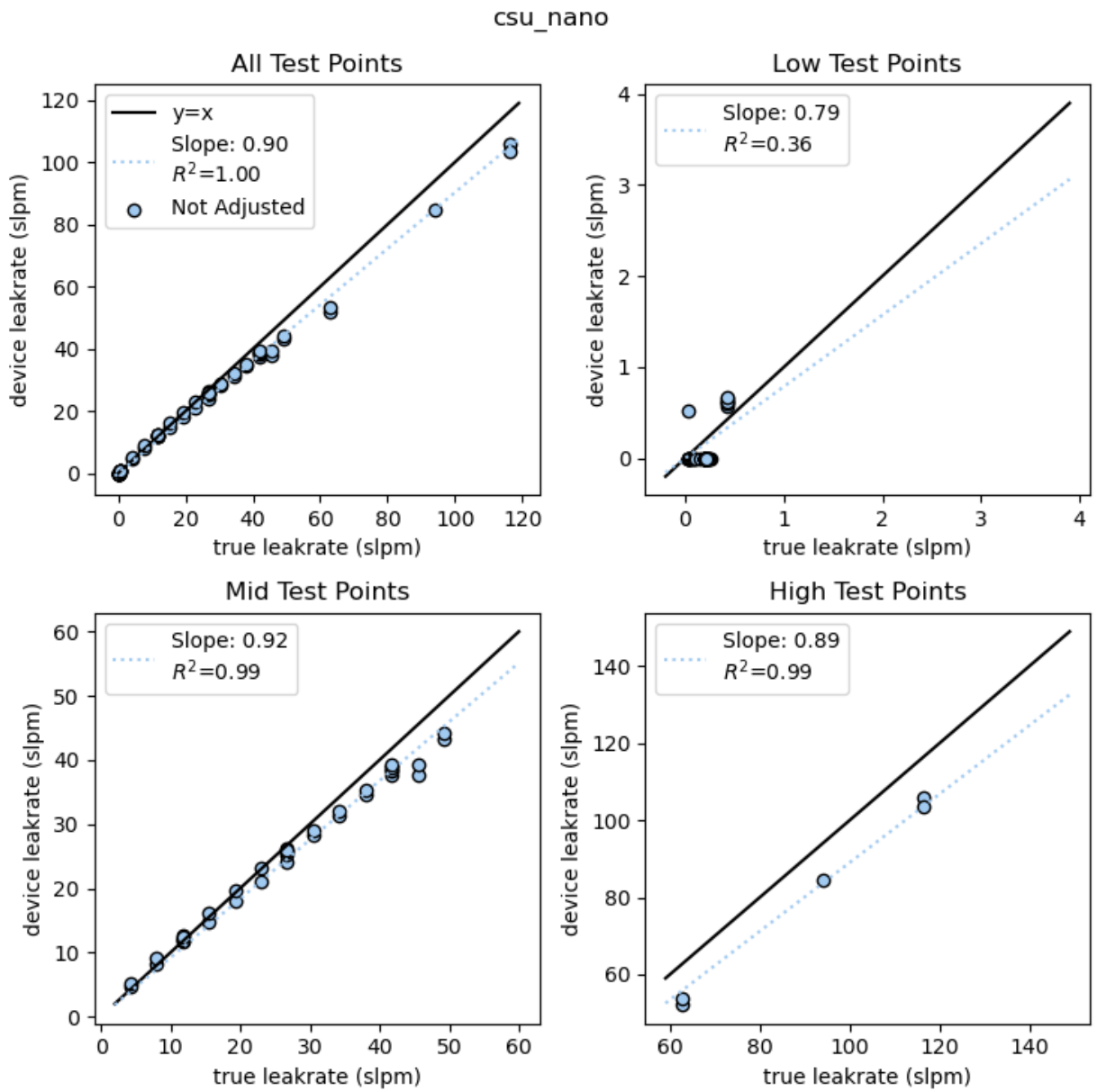

Figure 24: Prototype OS-HFS Nano sensor quantification accuracy.

Quantification accuracy tests were performed across the usable range of the prototype OS-HFS. Each emission rate was measured at two flow settings:

1) Emission rates lower than 30 SLPM used flow rates of 175 and 275 SLPM to improve sensitivity.
2) Emission rates greater than 30 SLPM used flow rates of 275 and 300 SLPM to ensure complete capture.

Four separate experimental setups were employed to generate "true leak rate" reference flows as a basis for comparison:

1) For the low test points (also included in LDL testing) leaks were generated using a critical orifice which was checked with a volumetric prover (Bios Drycal) before and after each test.
2) A dilute gas standard (2.5 % methane, balance air, Airgas Inc.) delivered by a mass flow controller (Alicat, Inc).
3) For the mid test points, 100 % methane (ME CP300, Airgas Inc) was delivered using a mass flow controller (Alicat, Inc).
4) For the high test points utility-delivered natural gas was metered using a thermal mass flow meter (Omega Inc).

Accuracy of both sensors was relatively poorly at low emission rates, although it should be noted that once the Nano began reporting values, they were very well correlated with the true leak rate. The Nano output switching behavior discussed in the LDL section can be seen in Figure 24 (top right panel).

Both sensors produced well-correlated linear responses in the mid test points, with good repeatability, though both were biased low. This result was unexpected based on the results of the sensor testing and flowrate testing and will be investigated further.

The INIR sensor became saturated for two of the three high test points and reported a 93 % leak concentration when the true leak concentration was 25-40 % for the three high test points. The high test points were conducted using utility-delivered gas with 85 % methane, 9 % ethane, and 1 % propane, while the sensor was calibrated using 100 % methane. This result highlights importance of considering gas composition, and the need for a built-in error checking to help alleviate similar issues in field deployed HFSs. The Nano sensor showed linear and repeatable results for the high range testing, although was biased slightly lower than for the mid-range testing.

Two additional accuracy tests were performed in December 2021 and February 2022 immediately following calibration of the INIR sensor, as shown in Figure 25. The results indicate that the INIR sensor had drifted since the prior accuracy testing was performed, and that the Nano had remained stable. Again, these tests showed a low bias in predicted leak rate from both sensors across the range of testing. The cause for this low bias remains unclear.

Taken as a whole, accuracy testing indicates that any productization of the OS-HFS design will require additional testing, and possibly control/calibration to maximize the accuracy of these sensors. While performance fell below expectations from earlier sensor-only testing, results indicate that:

- This class of sensor is capable of supporting an HFS instrument.

- Use of multiple sensors, using different sensing mechanisms, shows promise to identify errors, gas composition problems, or other accuracy issues that would not be caught by a unit using only one sensor or even multiple sensors of one type.
- Use of sensors with built-in A/D conversion and serial communication works well.

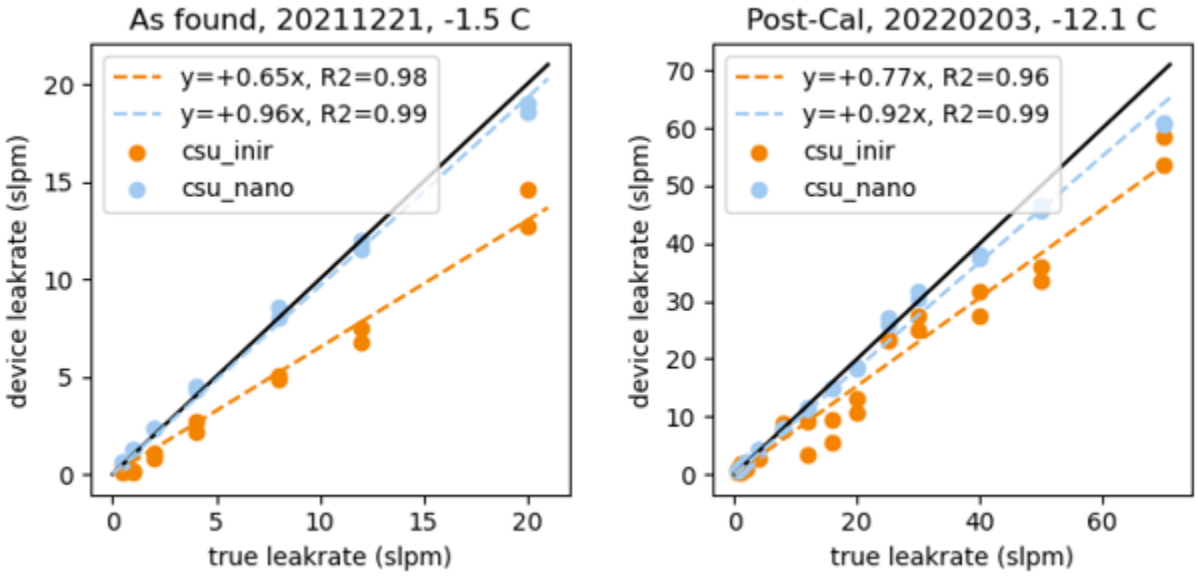

Figure 25: Additional Prototype OS-HFS accuracy testing results.

3.3.3 Gas Composition Testing

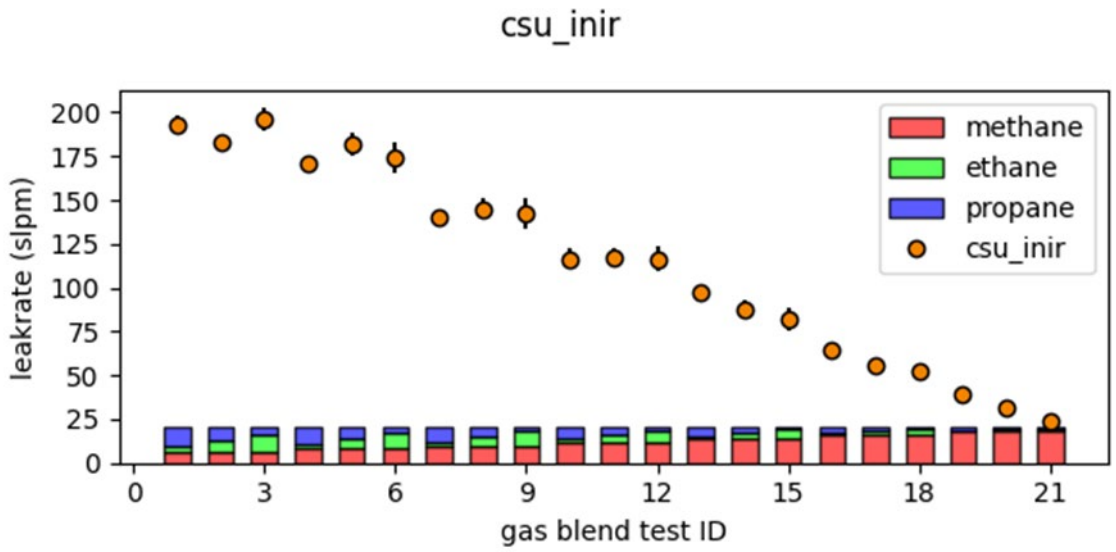

Figure 26: Prototype OS-HFS INIR sensor gas composition testing results.

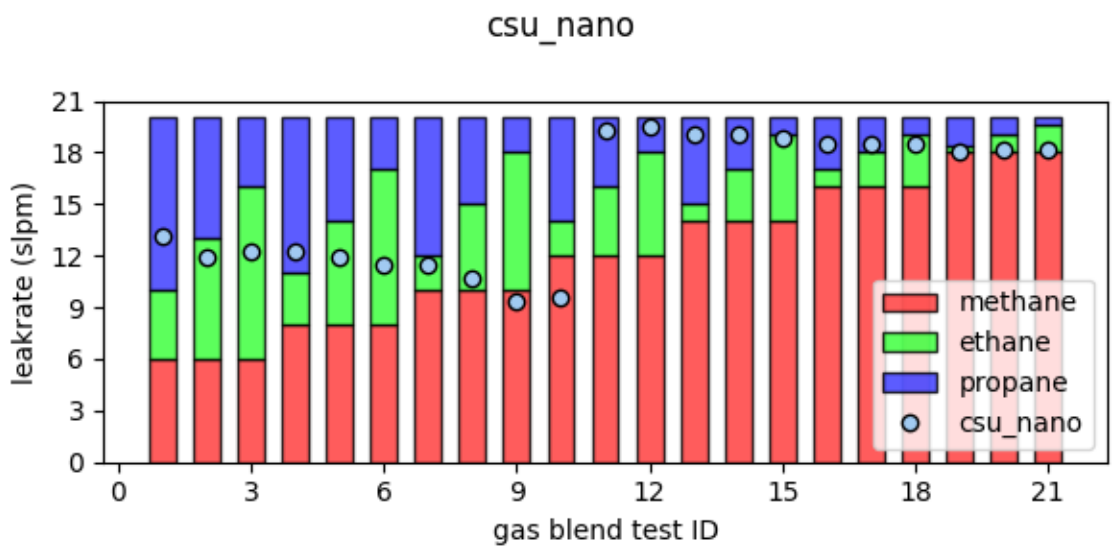

Figure 27: Prototype OS-HFS Nano sensor gas composition testing results.

For gas composition testing, 21 gas blends were generated with varying proportions of methane, ethane, and propane. For the OS-HFS, all blends were delivered at 20 SLPM. Three replicate tests were performed for each blend, varying the flow setpoint using nominal flows of 180, 240, and 280 SLPM.

The INIR sensor was calibrated with methane prior to testing and reported elevated emission rates for all blends with even a small amount of non-methane hydrocarbons (NMHC) present in the gas. The response increased dramatically with increasing NMHC content, illustrating the need for calibration on the gas under test for this type of sensor to avoid erroneous results and possible sensor saturation. The dynamic range of the sensor should be tested when gas blends with higher levels of NMHC are being measured to understand if, and at what level, the sensor becomes saturated.

The Nano sensor can differentiate between gas species, or blends of gas species, based on average molecular weights. For gas blend tests with a methane content less than ~50 % the Nano reported the presence of a "Light Gas" which is defined as a gas blend with an average molecular weight between 25-75 g/mol and a density between 1.2-2.5 kg/m^3, with a typical number of carbons between 1-4. For gas blend tests with a methane content greater than 50 %, the Nano reported the presence of "Methane" which is applicable to methane and light natural gas mixtures with an average molecular weight of 16-19 g/mol, average density of 0.6-0.9 kg/m^3, and typical number of carbons between 1 and 2. In this testing, gas test blends with an average molecular weight of 17-25 g/mol were reported as "Methane", and gas test blends from 25-33 g/mol were reported as a "Light Gas".

Over the range of gas test blends considered "Methane" the Nano, the output of the INIR sensor varied by a factor of five. When "Light Gas" was reported by the Nano, the INIR output varied by a factor of 2. This result indicates that an immediate accuracy improvement in reported emission

rate is not possible by applying a correction factor to the INIR data based on the gas classification provided by the Nano. Calibrating the INIR sensor on a gas other than methane would likely impact the results, although how much is not clear.

3.3.4 Practical Use Testing

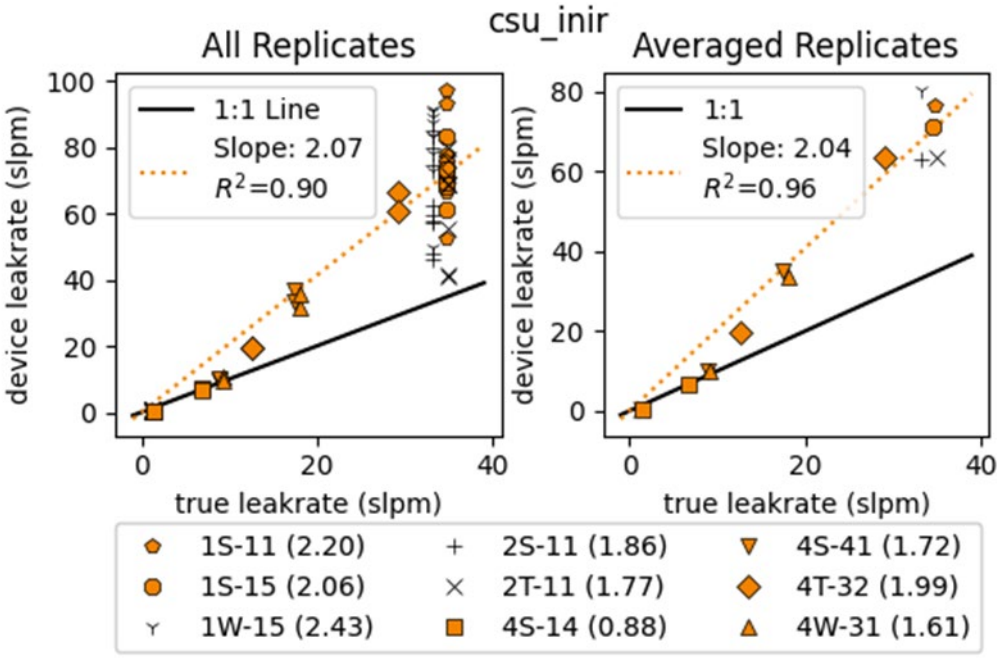

Figure 28: Prototype OS-HFS INIR sensor practical use testing.

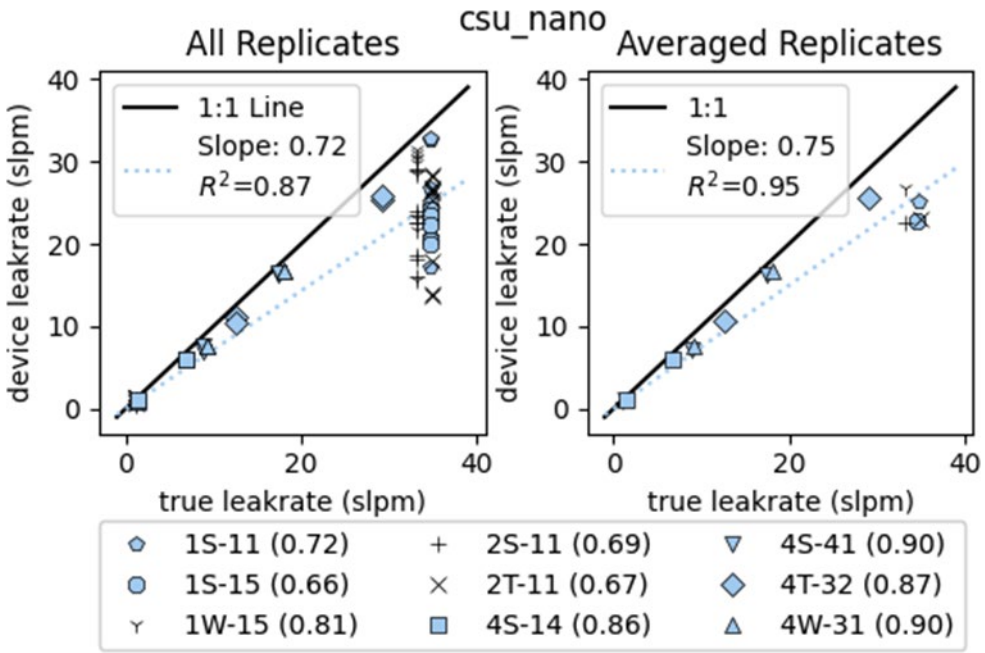

Figure 29: Prototype OS-HFS Nano sensor practical use testing.

For practical use testing, the prototype HFS was deployed in a mock field trial at CSU's METEC facility where its performance was evaluated against known emission rates on "real equipment" intended to closely mimic the challenges encountered in actual field use. Tests points with nominal true leak rates of 35 SLPM were tested on in early October 2021 (2S-11, 2T-11,1S-11, 1W-15, 1S-15) while the remaining emission points were tested in November 2021 while testing other pre-production HFS units. For the INIR sensors, all of the emission rates were overestimated due to the fact that the emissions were natural gas while the sensors were calibrated on methane.

For both sensors, the October test data shows a wide range of variability which may indicate that the challenges associated with field measurements (i.e., method accuracies) have a much larger influence on overall results than the instrument accuracy of the HFS itself. For the Nano sensor, all test results were biased low, though the overall bias was influenced by the October tests which showed a greater low bias than the November tests. These results further reiterate the importance of sensor calibration for the INIR sensor, but also indicate that performance from the Nano can be reasonable.

4. Testing of Pre-production Prototype HFS Units

In addition to the prototype constructed during this project, three commercial pre-production prototype units were also tested. The complete test protocol is provided in Appendix C, and a photo of the units is in Figure 30.

> **Note:** All pre-production units tested here were under development at time of testing. All test results should be considered preliminary, and readers are encouraged to consult the developers of these instruments for the most current performance data. Device descriptions are included as provided by manufacturers and specific claims have not been verified by CSU or CARB.

Four test sets were performed. The first three test sets (Sections 4.1-4.3) were performed by introducing the emission directly into the instrument by inserting the outlet of the gas release equipment into the inlet of the instrument. This approach ensures that all emissions were captured by the instrument. The final test (Section 4.4) measured representative leaks on real equipment. The final test was performed on modified field equipment at METEC at CSU. Five leak locations were captured and measured.

For all tests, instrument readings were recorded from the screen of the instrument. Data recordings produced by the instrument were reviewed but were not extensively analyzed. Code used to characterize the CSU prototype was also used to generate the analysis and charts seen below.

The following instruments were tested:

Figure 30: HFS units at METEC. Left to right: Sensors, Inc. (gas sensor module, handheld unit attached by cord), Bacharach HI FLOW, Hetek Flow Sampler, and the AddGlobe GFM.

- **Bacharach® – HI FLOW® Sampler: ("*BHFS*", herein):** This instrument was included for reference, as it is the most commonly utilized high flow instrument. Manufactured by Bacharach, it was recently discontinued and is no longer manufactured.

- **Sensors, Inc. – SEMTECH® HI-FLOW 2: ("*Sensors*", herein)**

  Sensors, Inc., 6812 State Road Saline, MI, 48176 USA

Description (from manufacturer):

•Sampler - Handheld device with a high-volume vacuum sampling fan and total flowrate monitor

•Analyzer - Portable control module (which can be carried, placed on the floor, or mounted to a backpack) housing the gas sensor technologies, control electronics, and battery pack

The combination of these two components (with a variety of sampling adapters) allows the entire fugitive methane emission to be captured, diluted, and quantified accurately.
By utilizing Tunable Diode Laser Absorption Spectroscopy (TDLAS) for the accurate measurement of the fugitive methane, the dynamic range for concentrations can accurately span 4 to 5 orders of magnitude and moreover without any cross-interference from other gases present in the captured leak. Coupled with an accurate measurement of the extracted flow (methane leak and ambient air) the volume- and mass-based leak rate of the fugitive methane can be determined with high accuracy over a wide range (for example 0.001 to 25 CFM).

Productization Plans: Q2 2022

- **HETEK Solutions, Inc. – Hetek Flow Sampler: ("*Hetek*", herein)**

  Hetek Solutions, Inc., 2085 Piper Lane, London, ON N5V 3S5 Canada

  Description (from manufacturer): The Hetek Flow Sampler is a portable, intrinsically safe, battery-powered instrument that accurately measures fugitive emissions in the field at natural gas components. This is accomplished by sampling at a large flow rate to completely capture all the gas leaking from the component, and by accurately measuring the flow rate of the sampling stream and the natural gas concentration within that stream. The gas leak rate is then calculated and outputted in a volumetric flow rate in either CFM or LPM. Hetek Solutions is pleased to produce the Hetek Flow Sampler, which serves to be the replacement of the discontinued BHFS, and support industry with an instrument that is made, serviced, and supported in North America.

  Productization Plans: Q2 2022

- **AddGlobe, LLC –GFM ("GFM", herein)**

  AddGlobe, LLC, 1650 Arabian Drive, Loxahatchee, FL 33470

  Description (from manufacturer): The Gas Flow Meter (GFM) sampler is a portable (9.3 lb., 290 x 285 x 100 mm), body made from high strength aluminum, explosion-proof,

battery-powered (Li-Pol) device designed to determine the rate of gas leakage from various pipe fittings and valves. Included in the device's capabilities are slide seals, compressor seals in trunk lines, storage facilities, compressor stations for natural gas, and many other sources of gas leakages. The product is 100 % modular. GFM is controlled wirelessly using an Android phone (version 6.0 or higher) that displays technical information and supervises the GFM sampler. The sampler is installed in a case that can be attached to a special harness, leaving the operator's hands free to perform measurements.

Productization Plans: The tested GFM instrument was a working prototype. Currently, the GFM 2.0 device is being mass-produced. The declared production volume is 50 devices per month. The new version (GFM 2.0) improves on the tested prototype, reflecting all the notes and comments from industry experts. This version of the device (2.0) is expected to be tested in a new independent study.

4.1 Lower Detection Limit

The primary purpose of this test is to identify the smallest leak size the instrument can detect, and if detected, report a measurement (which could be zero). To produce the small leak sizes required, the project team utilized regulators and precision orifices to control the gas flow and a precision meter (Bios Drycal) to measure the release rate. The test utilized industrial-grade methane. The emission was then introduced directly into the inlet of the instrument.

Where possible, the release rates were varied from below LDL (instrument reports false negative detections all the time) to solidly above the LDL (instrument reports true positive detections all the time). To determine the LDL, a logit curve was fit to the data (scipy.optimize.curve_fit library) and used to compute the LDL. Results are shown in Figure 31 through Figure 34, in alphabetical order. The right plot in each figure shows the points used for the logit regression, and the legend indicates the 50 % confidence LDL computed from the logistic regression. Comments follow the figures.

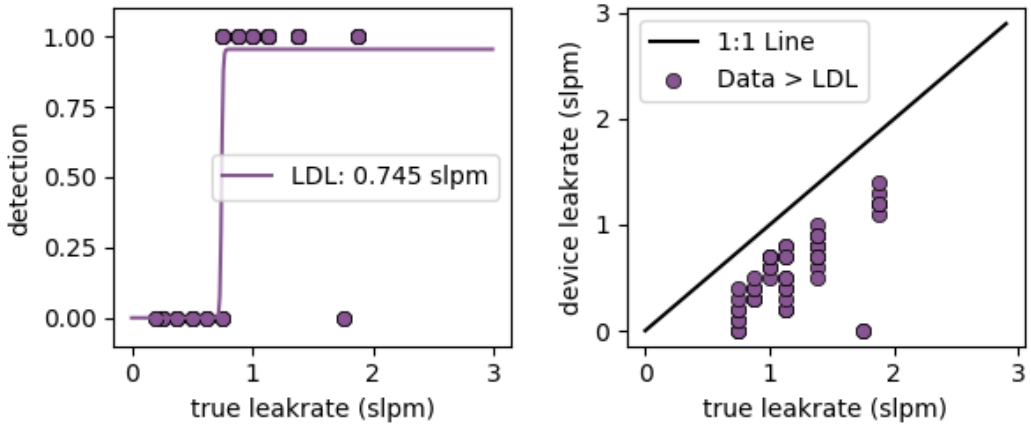

Figure 31: BHFS lower detection limit.

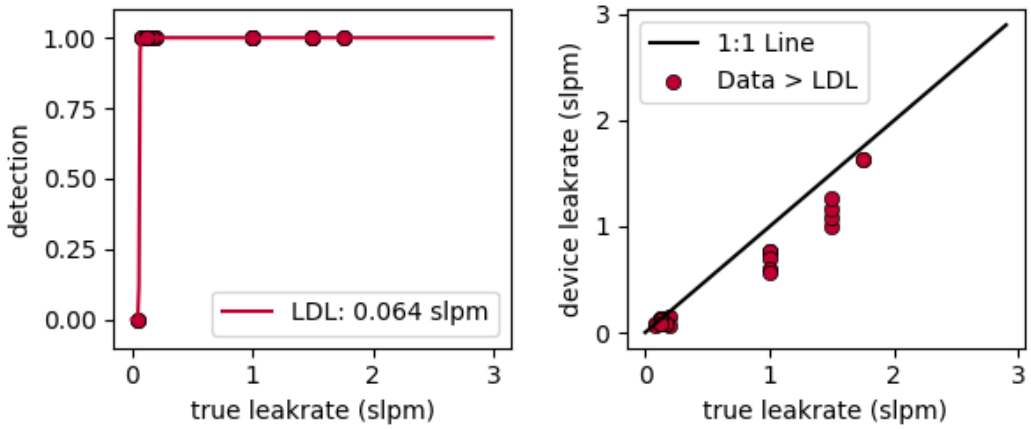

Figure 32: GFM lower detection limit.

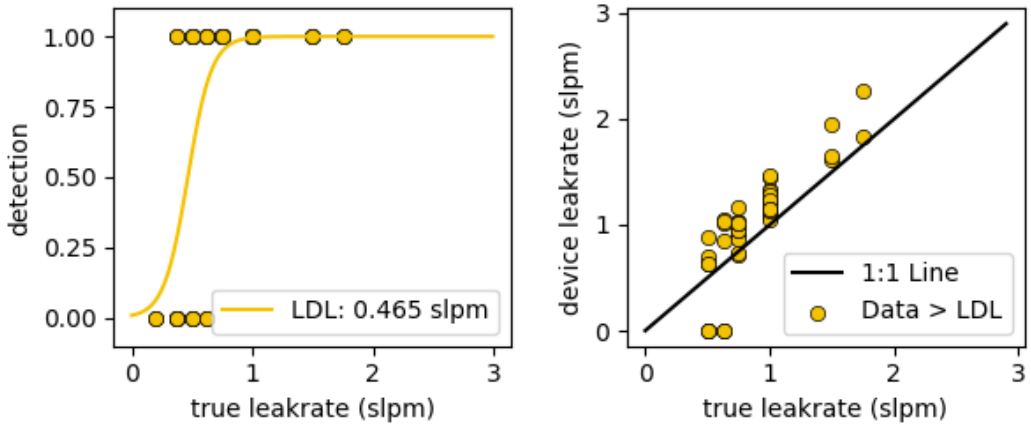

Figure 33: Hetek lower detection limit.

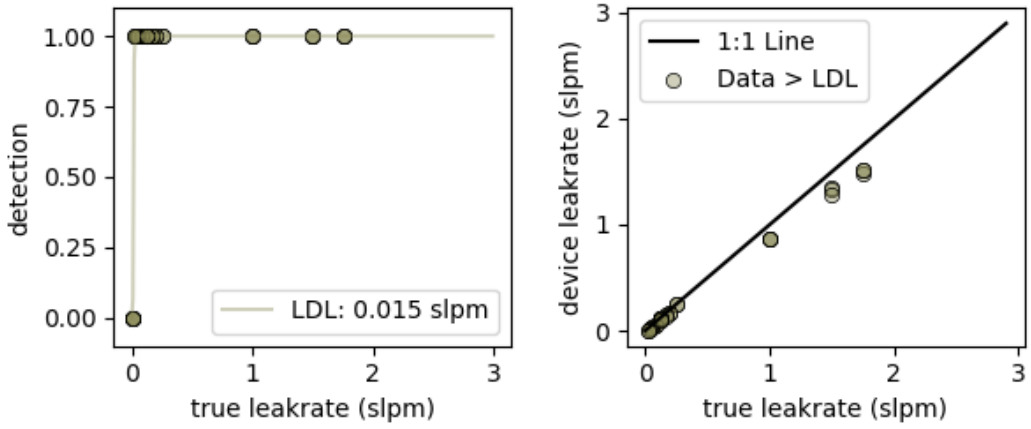

Figure 34: Sensors lower detection limit.

LDL varies substantially in these pre-production units, and likely reflects different design points for the companies. LDL for the BHFS unit in this more-rigorous testing is substantially higher than

the 0.2 SCFH (~0.1 SLPM) LDL measured in Zimmerle et al. [25], and shows a low bias at low flow levels. For the new products, LDL ranged from a low of 0.015 SLPM for the Sensors unit to 0.47 SLPM for the Hetek unit – a difference of 30x. All showed less measurement bias at these low emission levels than the BHFS unit.

Suitability of any LDL is likely a function of the sector in which measurements will be made; leaks in distribution systems (e.g., residential meter sets) tend to be smaller than those in midstream or upstream sectors.

4.2 Quantification Accuracy

The primary purpose of this test is to characterize the quantification accuracy of the instruments when measuring industrially pure methane. Release rates were varied from above the range used in LDL testing to the maximum upper limit of CSU's release equipment*.

Results are shown in Figure 35 through Figure 38. Because several instruments show markedly different performance at different release rates, data in all figures has been split into four panels. The upper left panel shows a least-squares fit through all of the data, across the entire range used for the test. Upper right shows only test points below 4 SLPM, lower left data for the mid-range of 4-60 SLPM, and lower right data above 60 SLPM.

Since all units were pre-production at the time of testing, companies were provided a chance to review and respond to the data prior to publication. Two companies responded with explanations for certain errors that the project team deemed were valid. Adjustments based on companies' explanations were applied prior to analysis. Plots are marked with circles if the data was not adjusted due to company input, and squares if it was. Adjustments applied to the data were:

1) Hetek Solutions, Inc. indicated they had found a firmware error, where measurements above 65.536 LPM would display incorrectly. They provided corrected values, which were included in the analysis.
2) Sensors, Inc. indicated that a calibration error was causing the unit to read 5 % low. A uniform +5 % was applied to all non-zero data points.

* In principle, the instrument can be tested at leak rates up to the point that the instrument reported saturation on the highest blower speed. In practice, this did not occur during the testing performed here. Maximum concentrations observed in this testing were:

Unit	Maximum Gas Concentration (%)
BHFS	45.0
GFM	55.0
Hetek	78.4
Sensors	28.7

In general, curve fits across all data or mid-range data sets are likely to be the most representative of measurements in the field, except for cases where most emission points are extremely small or large.

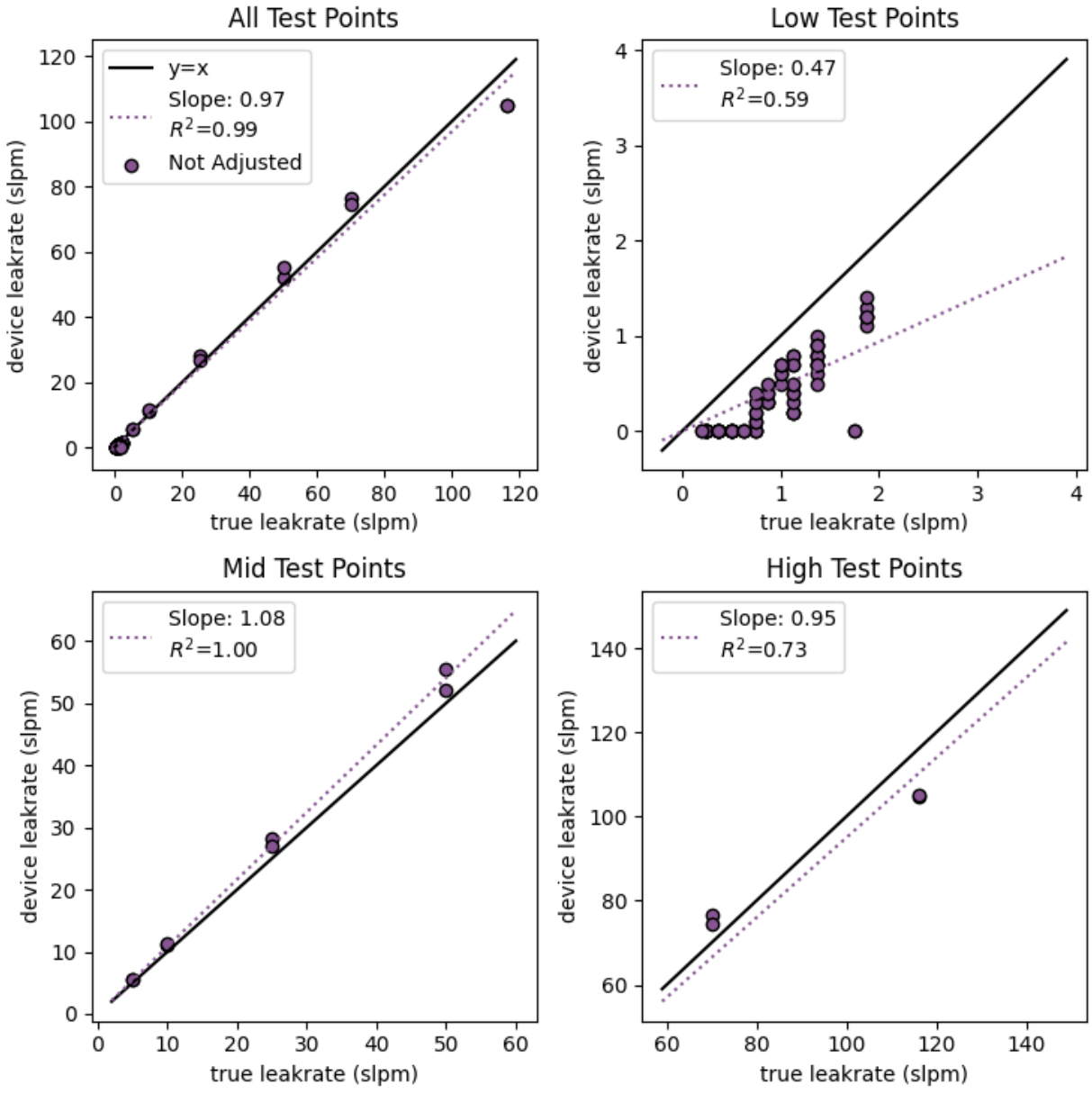

Figure 35: BHFS quantification accuracy.

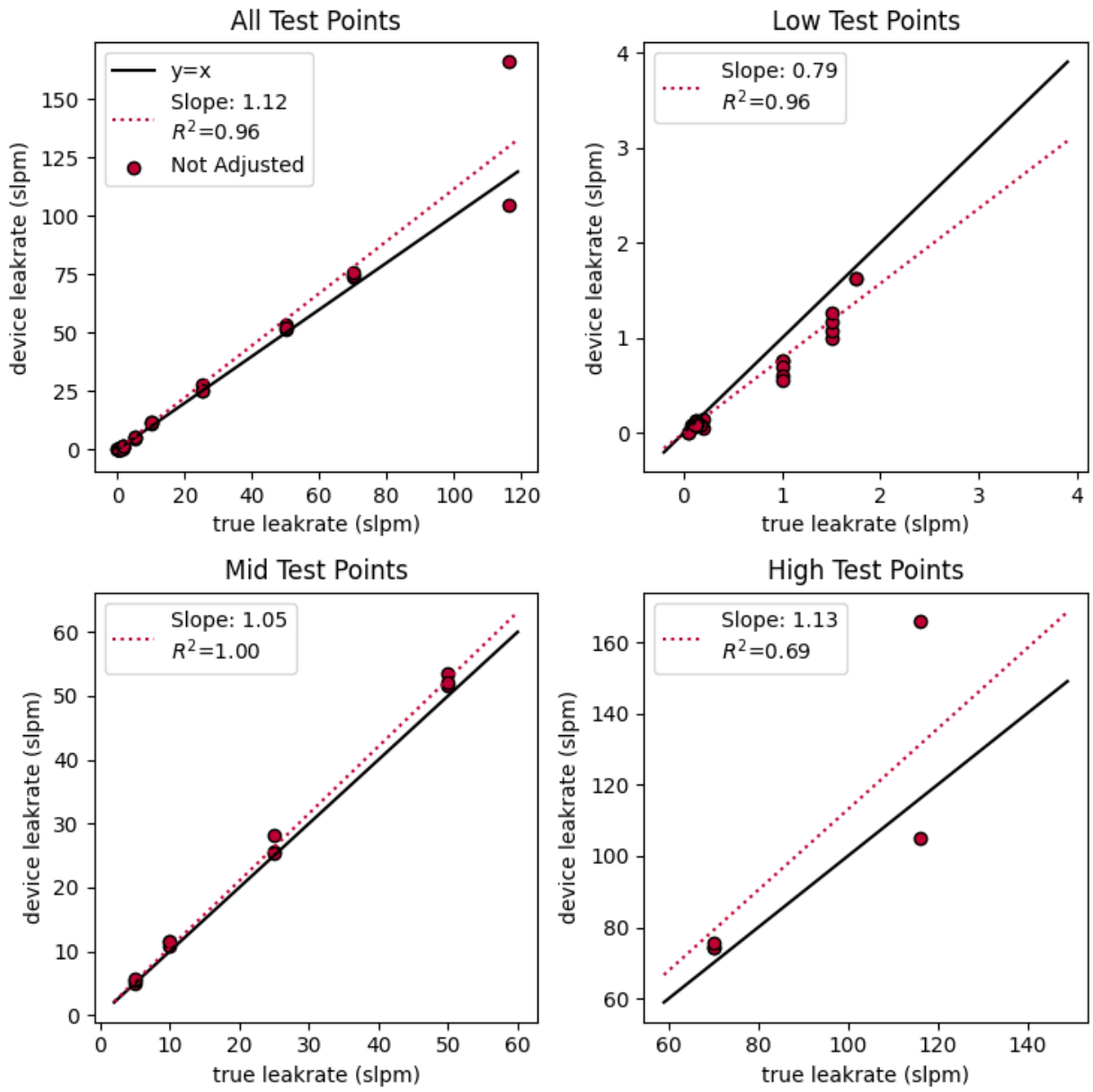

Figure 36: GFM quantification accuracy.

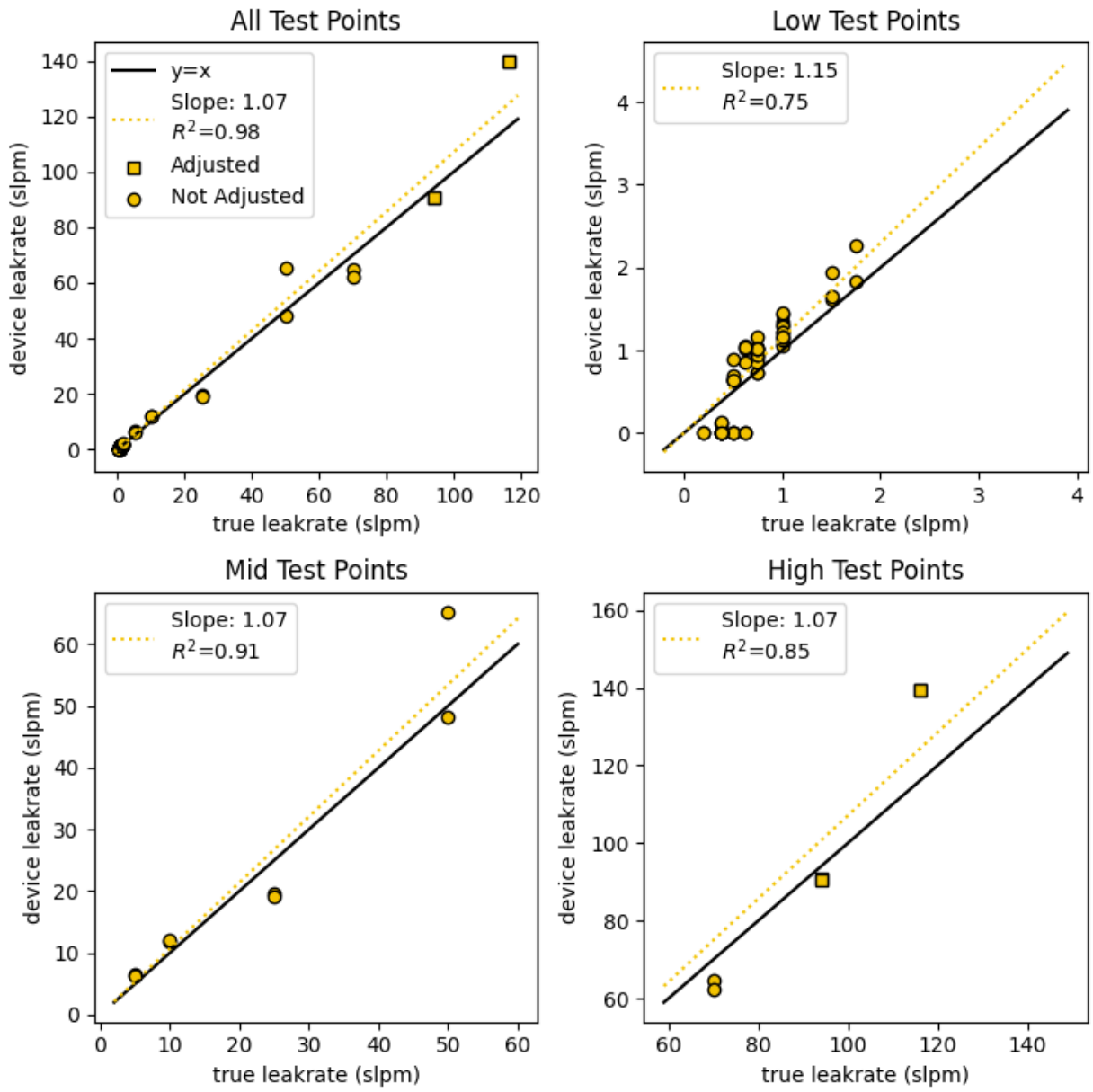

Figure 37: Hetek quantification accuracy.

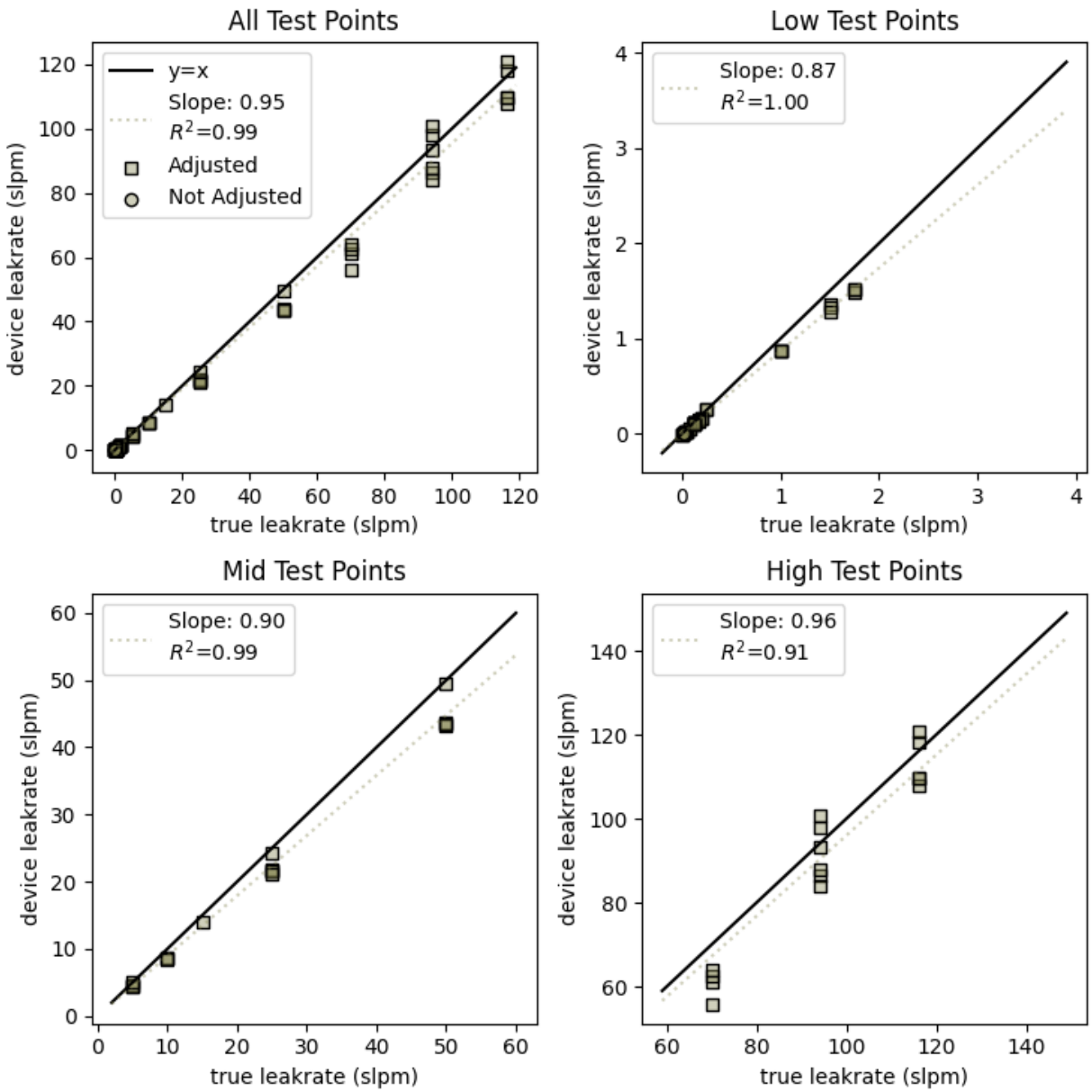

Figure 38: Sensors quantification accuracy.

For the testing performed here, all prototype units showed some bias (slope of the curve fit), which is likely due to the pre-production status of the instruments; no fundamental performance problems were uncovered during testing. In the middle range testing, biases run from -10 % to +8 %, with somewhat higher biases observed for the high range. For the low range – using the same data as for the LDL test, but with all points, including non-detects included – bias is, as expected, substantially higher.

4.3 Gas Composition Testing

The primary purpose of this test is to understand how the instrument reacts when gases other than methane are introduced into the instrument. Traditionally, high flow instruments were designed for market natural gas that contained primarily methane with 0-15 % (typically 0-5 %) ethane and small quantities of other gas species. In the last decade HFS measurements have been increasingly conducted in upstream (production and gathering) systems, where gas mixtures contain higher NMHC fractions, and gas compositions vary more between facilities and locations within a facility.

The primary commercial instrument, the BHFS, is calibrated on methane and methane diluted in dry air. Correction for other gas mixtures, or calibration on those mixtures, is possible by following hints in the manual and having an understanding of the sensors used in the instrument. In practice, these corrections have been challenging[25,26] and often require taking supplementary measurements, such as gas samples for speciation with gas chromatography.

The other instruments arrived calibrated, and calibration was attempted on all units, as per common practice, although calibration instructions were not complete for any of the instruments. Additionally, the internal gas concentration sensors vary in their sensitivity to other hydrocarbon gases. While some are largely methane-specific, others utilize sensors which respond to all combustible gases (e.g., catalytic oxidation sensors) in the gas stream.

> **Note:** Gas composition tests should be seen as an indicator of what controls are required to use the instrument with gases containing significant NMHC, rather than as a specific performance metric for extracting either methane or total hydrocarbon emission rate from measurements. Practitioners are advised to follow instructions from the manufacturers.

Testing was performed by varying the mix and release rate of methane, ethane, and propane in the emission. Mixing was performed using the METEC gas mixing rig (abbreviated “GMR” in the attached data files). Results are shown in Figure 39 through Figure 42. Limited data is shown for the BHFS unit, but additional results can be found in Zimmerle et al.[25]

Each of the plots shows a stacked bar representing the gas mixture for each test, in volumetric units. The lowest bar is methane, and a methane-specific instrument should produce measurements located at the top of this bar. Measurements are shown as points with error bars derived from repeat measurements performed for each mixture.

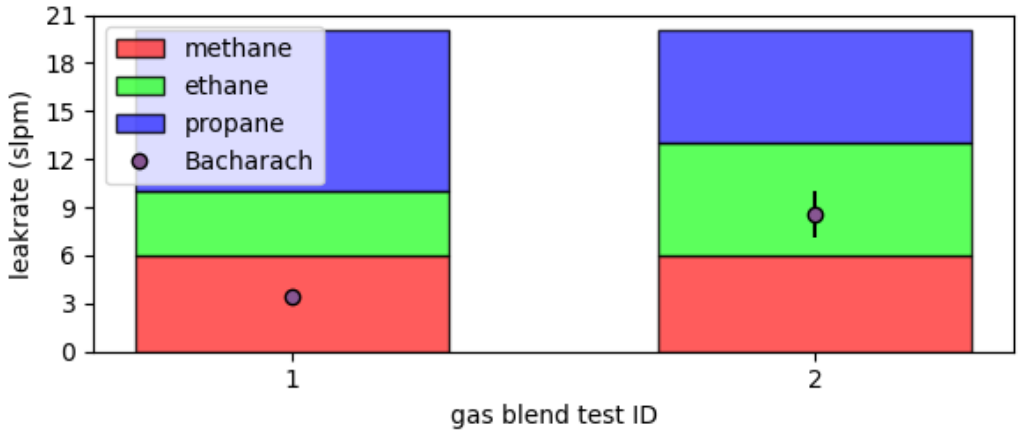

Figure 39: BHFS gas mixture results.

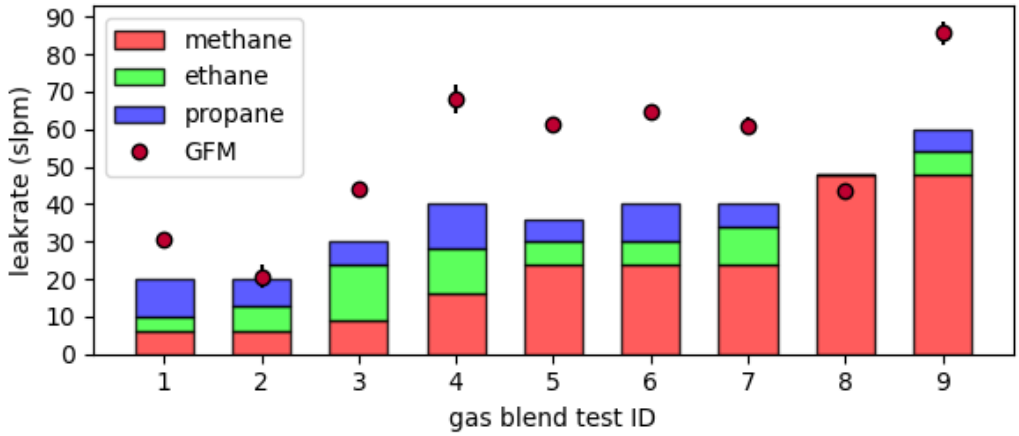

Figure 40: GFM gas mixture results.

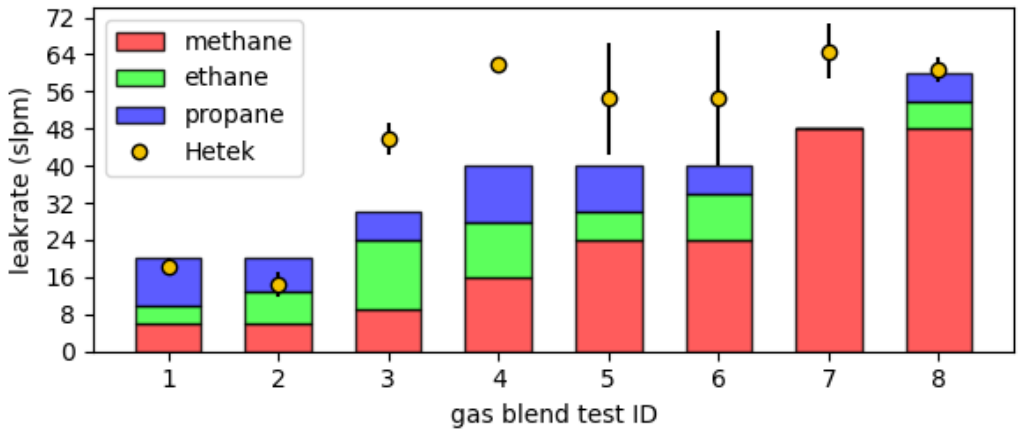

Figure 41: Hetek gas mixture results.

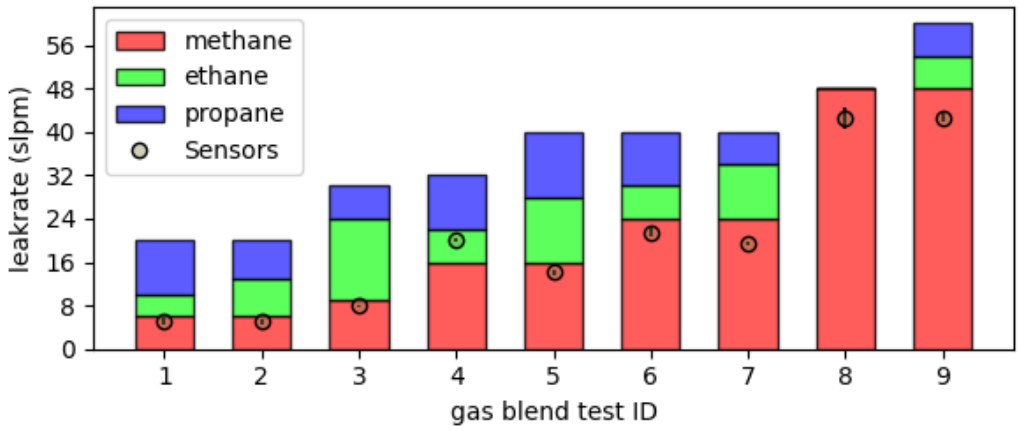

Figure 42: Sensors gas mixture results.

As noted earlier, the sensors embedded in each instrument may have substantially different sensitivity to NMHC. For example, the catalytic oxidation sensor in the BHFS unit is sensitive to all combustible gases, and for gas streams with appreciable NMHC, corrections must be performed.[26] The Hetek and GFM instruments show similar deviation when NMHCs are introduced, while the Sensors instrument exhibits behavior that is more methane-specific.

As noted in other sections, all of the tested instruments are pre-production units. Guidance for gas streams with a high proportion of NMHC gas species, specialized calibration, and other usage guidance was not available at the time of testing.

4.4 Practical Use Testing

The primary purpose of this test is to determine if the instrument configuration will impact the ability of an operator to enclose and measure a leak. To perform this testing, the test operator utilized the instrument to measure a variety of leaks at METEC, noting how accurately the leak rate was measured, and any issues with operation of the instrument. For this testing five locations on Pad 4 at METEC (Figure 43) were utilized as representative equipment.

Figure 43: Pad 4 at METEC with equipment groups marked.

The test locations are known by their METEC identifiers (photos in Figure 44):

- 4S-14: Fitting on a temperature controller on a three-phase separator.
- 4S-41: Pressure relief valve line on the doghouse of a three-phase separator.
- 4T-32: Thief hatch on tank 4T-3.
- 4W-31: Valve packing on a large casing valve on a wellhead.
- 4W-32: Flanged connection on the wellhead casing.

Following the recommended protocol for high flow measurements (Appendix B), measurements at each location/leak rate combination were completed with multiple total flow rates through the instrument. See data files for details. Replicated measurements made at different flow rates are identified as "replicates" in descriptions below.

Data for the Sensors, Inc. instrument was adjusted as described in the quantification section (Section 4.2), and plots contain a notation to indicate the adjustment. Data for the Hetek Solutions, Inc. unit *was not* adjusted as described in Section 4.2.

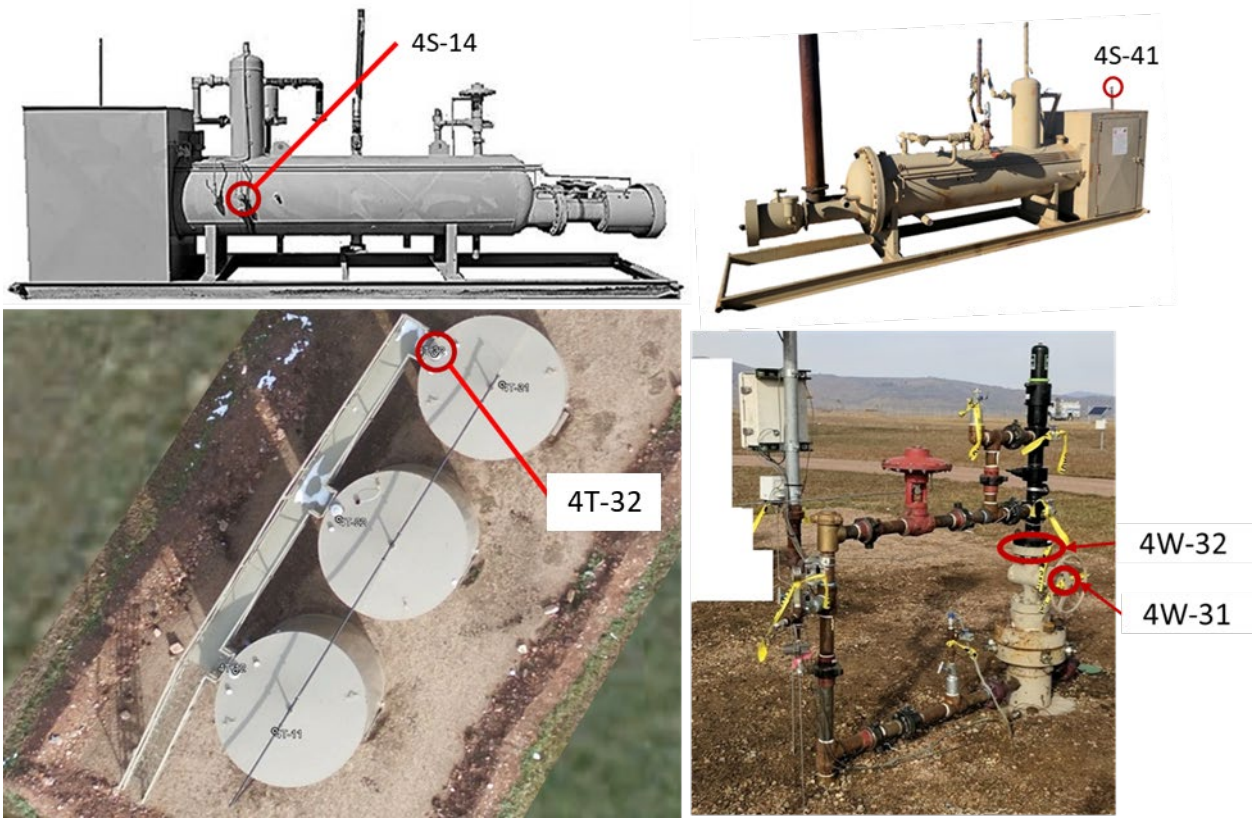

Figure 44: METEC release points used for testing.

Results are shown in Figure 45 through Figure 48. In each figure, the left panel illustrates all measurements made on the selected leak points, while the right panel presents the same data after all replicates for each emission point location and emission rate have been averaged. In practice,

multiple leak measurements are typically averaged prior to use in a study. Linear fit through the data was done with ordinary least squares, with no intercept.

The panel legend on the bottom of each figure provides the leak location identifier, as per the list above, and the ratio of measurements to true leak rate in parenthesis for each emission point. The ratio is calculated as:

$$r_j = \frac{\sum_{i=1}^{N_j} M_{i,j}}{\sum_{i=1}^{N_j} A_{i,j}}$$

where subscript j refers to all data for one test, with a "test" being defined as one emission location at one nominal leak rate. r_j is the ratio for test j. $M_{i,j}$ and $A_{i,j}$ are the measured and actual emission rate for the i^{th} replicate for test j and N_j is the number of replicates for that test.

To perform the test, the leak location was bagged once (similar to Figure 5), and then each instrument was used to measure the bagged location by swapping the hose to the instrument. Therefore, all instruments utilized the same leak capture.

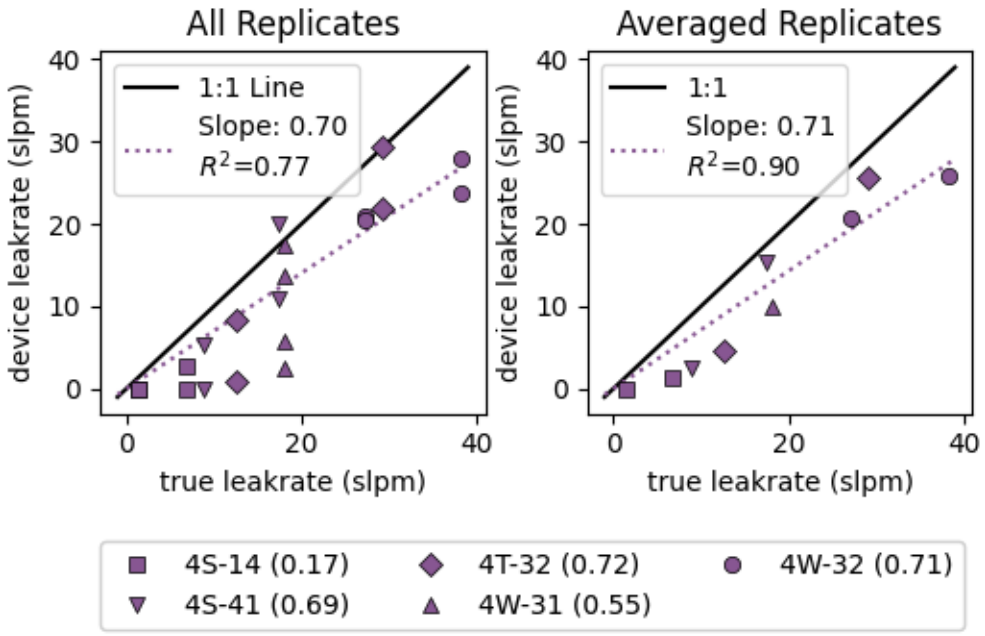

Figure 45: BHFS practical use testing.

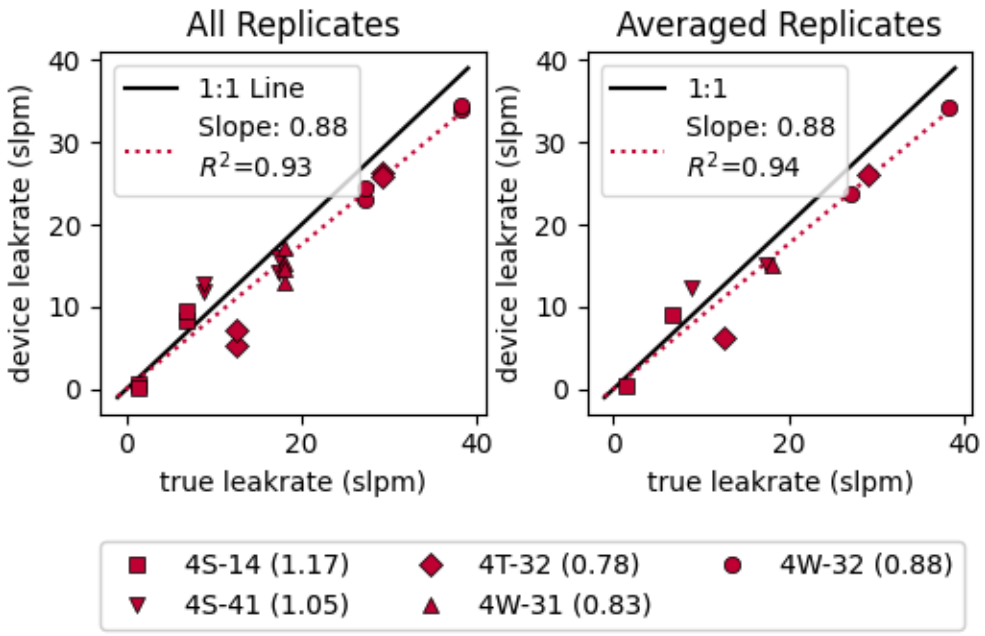

Figure 46: GFM practical use testing.

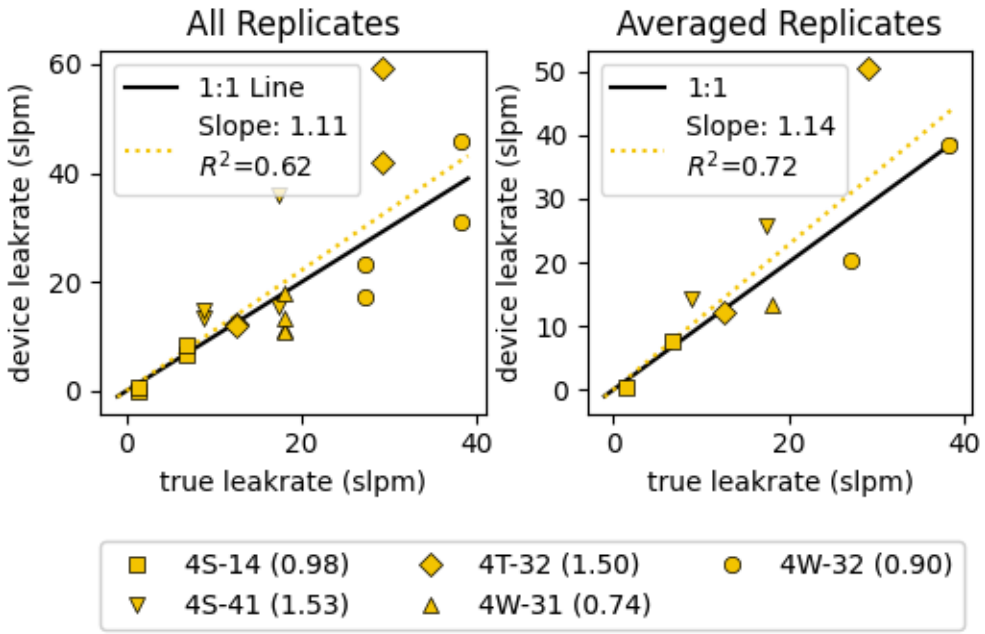

Figure 47: Hetek practical use testing.

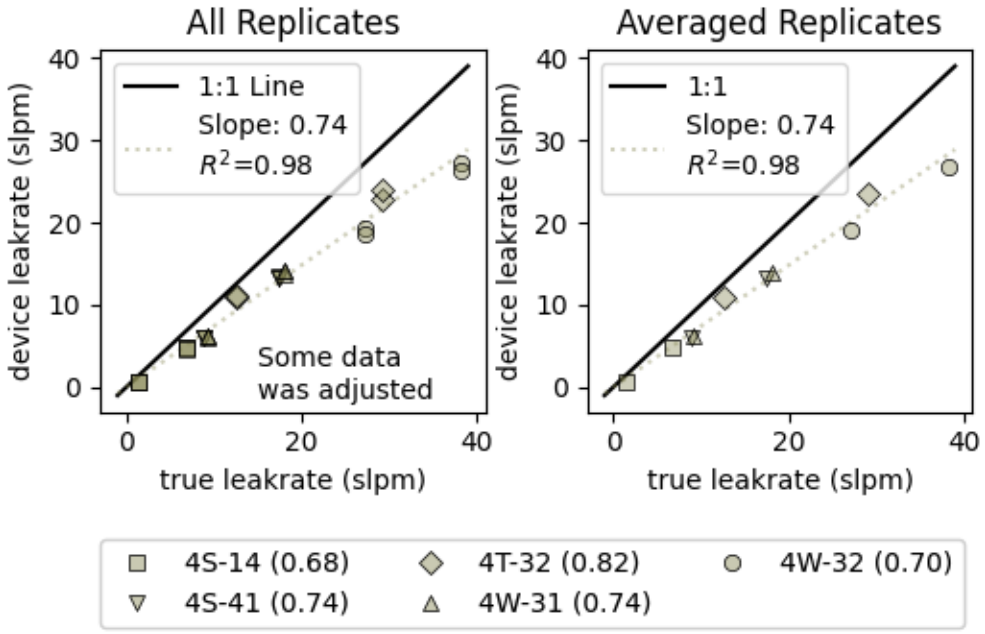

Figure 48: Sensors practical use testing.

In this category of testing, a useful comparison is between the widely utilized BHFS instrument and each of the other three instruments. As can be seen from the plots, both errors and bias increase when applied to realistic emission points relative to the results in Section 4.2, where emissions were introduced directly into the inlet of the devices. This test combines factors due to the instrument performance – ease of use, range of flow rates, etc. – and factors that are independent of the instrument and primarily dependent on the high flow method itself – primarily variability in capturing the leak, but also changes in back pressure and other factors which can disturb measurement accuracy.

A key element for evaluating instruments is the range of results for any one test – i.e., device leak rate variation for one true leak rate (X axis). The pre-production instruments differ substantially in this area, and this is an area for attention during product finalization.

4.5 Testing Summary

Performance testing of these pre-production units indicates that the new units are on track to be capable of replacing the BHFS instrument in the field. The units demonstrate different "design points," with variations in lower detection limit and, likely, upper quantification limit. For this testing, quantification was limited by the available equipment, and the upper end of several instruments was not fully characterized.

As pre-production units, additional work is required on most units. Key elements include:

1) Improve instrument accuracy, and by association, clearly document calibration procedures or calibration confirmation procedures if field calibration is not required. Most of the instruments show some type of offset – unsurprising given the pre-release status of the instruments – that can likely be corrected with sensing and software updates.

2) Decide on, and communicate, procedures for handling gas streams with a high proportion of non-methane components. Procedures will likely be instrument-specific and could vary between avoiding certain gas compositions to specific correction instructions.

Additionally, most units still require final safety qualification prior to release; this was not an issue for the testing.

Testing results also highlight the need to standardize testing of these instruments. Recommendations include:

1) Structure testing to capture multiple replicates at each test condition to better characterize the instrument stability and accuracy.

2) If possible, test more than one production unit to evaluate inter-unit variability (as has been seen on some BHFS units[25]).

Finally, the test results illustrated (again) that the uncertainty in high flow field measurements is likely underestimated due to challenges in measuring real equipment in field conditions.

5. Conclusions and Recommendations

In general, topic-specific recommendations are included throughout the report. This chapter discusses only major points from throughout the report.

5.1 Key Conclusions: CSU Prototype OS-HFS

The CSU prototype OS-HFS unit represents a fully functioning, although incomplete, prototype of a high flow instrument. Key design elements have been integrated and tested, including:

- Use of commercial, off-the-shelf, components for key physical and sensing elements, including use of a widely utilized blower with integrated speed control, a commonly available high-energy battery pack, and a commercial enclosure as a water-resistant case for the instrument. All of these factors increase the chance that a reader could create a working unit and do so with minimal investment.

  An exception to this improvement was the hose and enclosure appurtenance (also known as "the bag", but potentially including several elements to capture emissions in different leak geometries) required to capture leaks in field conditions. The project team found no good substitutes for the existing commercial vacuum cleaner hose and the bag used with the BHFS unit. This is definitely an area for further investigation and development.

- The prototype demonstrated a new architecture for a high flow instrument by using a commercial SBC (Raspberry Pi) for control, user interface, and data management purposes, and – most importantly – loosely coupling that computer to the rest of the instrument. To use this type of generic computation device in an instrument required three crucial design decisions:

  - All sensors are read using serial communications – industry standard UART or I2C interfaces – that are readily supported by most SBCs. The computer performs no A/D conversion directly (onboard A/D converters on SBCs and microcontrollers have low resolution and are notoriously inaccurate). Additionally, the required A/D conversions are isolated from the high-frequency, high-noise, computation and display circuitry.

  - Using a standard, interpreted, language (Python) for data acquisition, control, and display purposes. A platform-independent language supports replacement of computer and display as needed by minimizing specialized microcontroller software tools and associated hardware dependencies.

  - Keeping the control computer separate from the printed circuit boards supporting sensors and other data acquisition.

- Driving the display using an industry-standard HDMI interface.

These design decisions effectively isolate the instrument's computer from the sensors and measurement circuitry in the instrument. Innovation in, and obsolescence of, the computer element of an instrument occurs far faster than that of sensors or other hardware components. Additionally, installing software updates to correct problems after the instrument is released is a robust process that is readily accessed by users.

Adopting this approach will make high flow instruments more adaptable as needs change and expectations for data handling and communication evolve.

- Sensor manufacturers are rapidly moving toward sensors which include A/D conversion inside the sensor, often including additional corrections that allow the sensor to be more stable and operate over a wider range. Performing A/D conversion in the sensor also reduces susceptibility to electrical noise inside the instrument. The OS-HFS used an analog sensor only for pressure (with dedicated A/D converter chip); all other sensors had integrated A/D conversion and serial communications. The prototype demonstrates that serial communication is sufficiently fast and robust for high flow applications.

- The exclusive use of serial communications also allows the CSU prototype OS-HFS to demonstrate, if not fully implement, a sensor-independent architecture. Improved sensor variants can be swapped into the instrument as sensors evolve, likely requiring only minor updating of communication code if similar sensing is performed, as would be common when using sensors from the same manufacturer. Since many high sensitivity instruments (e.g., trace gas analyzers) also utilize serial communication, this approach also supports the integration of such an instrument as a sensor for the high flow process by writing a new "reader" for the instrument. This type of integration could be useful if measurements require higher sensitivity (e.g., for very small leaks), better gas speciation, or sensitivity to specific gas species.

  The prototype demonstrates the concept of a sensor-flexible *high flow platform* that could adapt to new uses and challenges as they arrive.

5.2 Key Conclusions: Pre-Production Prototype Instruments

While several pre-production instruments were tested as part of this project, it is important to note that, for the most part, the instruments did not leverage the architecture developed during the project. That said, all instruments utilize the HFS measurement method, and make no major break with the high flow method as it has been practiced since the 1990s.

Certain features of the CSU prototype were represented in some of the pre-production instruments – most often cases of convergent design, but possibly including leverage from discussion of early work on the project. Examples include:

1) Modernizing the user interface and data collection of the instrument relative to the BHFS instrument. Based upon field experience, the CSU prototype moved the display from a corded tether to the top of the instrument unit, where it could be read top-down while working. Several pre-production units also addressed this need with remote displays (GFM, Sensors) that were not tethered to the unit.

2) Two of the pre-production units (Sensors, GFM) opted for instrument configurations that differed substantially from the BHFS – generally smaller packages that were more readily positioned by an operator during measurement. The GFM unit utilizes a similar package style as the CSU prototype, while Sensors, Inc. developed a radically new handheld design. In contrast, Hetek chose to closely mimic the BHFS backpack configuration.

   Despite progress in this area, use model and associated ergonomics remain challenging in field conditions; these instruments are still bulky and heavy for use in the field, particularly since no unit – CSU included – identified more compact or lighter weight hoses and enclosures for capturing the leak.

3) Field experience indicates that it is very useful to log high-speed sensor data underlying the computed leak rate for later post-processing to identify issues or better characterize uncertainties. The CSU prototype prioritized this feature, and most pre-production units also included data logging, although not all were readily accessible at the time of testing.

However, none of the instruments included several key elements identified during this work:

1) Support for multiple complementary sensors. Practical experience in the field has shown that it is operationally challenging to correct for different gas mixtures in field conditions. The intent of the CSU prototype was to support one sensor as the primary measurement sensor (SGX INIR sensor), and a second sensor (Nano) with different response to gas mixtures, allowing deviations in gas mixture to be detected, even if a composition-dependent correction was not possible without more information.

2) Recent field campaigns and laboratory experiments indicate that the “background concentration sensor” is not necessary in the vast majority of measurement conditions. Therefore, the CSU prototype unit did not include a background sensor, while several pre-production units did.

   While the presence of a background sensor appears to be positive, in practice, the background sensor is often hard to isolate from the leak point’s emissions, draws in elevated

emissions that *are not representative of true background,* and results in decreased emission rate estimates. This is highly undesirable. In the opposite extreme, measurements are seldom conducted, for safety reasons, where the background concentrations are substantially elevated. Therefore, a background sensor tends to occasionally underestimate, and only rarely overestimate, emissions. In the judgement of the project team, it is not worth the additional cost and complexity to add a second sensor for background characterization.

An ongoing problem with the BHFS has been the difficulty of measuring emissions with varying methane content – either to produce a methane emissions number, or to properly characterize a total VOC number. With the exception of the Sensors instrument, which is methane-specific, the vendors need to be clearer about how to handle emissions with varying gas composition during both calibration and field use.

5.3 Key Conclusions: High Flow Method and Instrument Testing

Finally, development and testing conducted in this project highlight several areas that require additional attention:

1) Measurements conducted here on "real equipment" at METEC suggest that the uncertainties related to the high flow *method* (as opposed to the instrument) may be under-estimated in field conditions. Testing performed here, and other informal testing completed at METEC, illustrate that incomplete capture (or other stressors on the measurement process) tend to increase inaccuracies and potentially add bias to measurement results.

   Additionally, testing at METEC tends to be less complex than true field conditions: Equipment is not heated, there is generally less time pressure, and the objective of the test is clearly known, stimulating best practices by measurement personnel. Therefore, it is likely that the uncertainties seen in Section 4.4 represent a lower bound on true field uncertainties.

   The project team recommends that these uncertainties be characterized, using professional measurement staff in a controlled, but realistic, environment.

2) Production units should undergo testing similar to what was conducted here prior to field use. All units exhibited problems of some nature – all likely fixable – but additional testing would raise confidence in these instruments for future use.

3) To support testing, there is a need to further standardize protocols for testing the instruments, and likely a need for a lightweight protocol to check performance in the field. This testing should be structured to capture multiple replicates at each test condition and ideally test more than one production unit to evaluate inter-unit variability (as has been seen on some BHFS units[25]).

The high flow method remains one of the few methods suitable for isolating individual emission points for direct measurement. Quality instruments in this area are the key for characterizing emissions from components or other ‘point’ locations. This type of quantification produces critical information for leak detection and repair programs, helps with development of equipment- and component-specific emissions factors, and generates actionable information for emissions control programs.

Appendix A Data Files and Additional Materials

Description of each data file, file name, contents.

- Consolidated.xlsx – Test results from the prototype OS-HFS and pre-production HFSs from all three manufacturers, plus the reference BHFS.
- OSHFS Software v1.zip – all software used in the prototype unit. The software contains several screens that were not fully implemented in the prototype, but are retained in the distribution as examples, and to avoid last-minute changes which may break the software.
- HiFlow_Assembly_V7 v7.iges – IGES solid model files for the mechanical assembly.
- Gas_sensor_mount PCB.zip – board design files for the sensor PCB (only custom PCB build during the project).
- Part Datasheets.zip – Manufacturer data sheets for key components, including the INIR and Nano MPS sensors.

Appendix B Recommended High Flow Method

B.1 Purpose

The purpose of this document is to outline a protocol for making a complete high flow measurement in field conditions. This protocol provides a quality control mechanism for high flow measurements which can be referenced by companies, regulators, or other interested parties. The protocol is not instrument-specific, although instruments may automate parts of the process to assist users of the instrument.

Prior to starting this protocol, the instrument must be properly calibrated and powered, following instructions for the specific high flow instrument; calibration and maintenance procedures are not included in this protocol. Additionally, the accuracy of the measurement is a function of both the measurement protocol, described here, and the instrument making the measurement. Individual users must estimate errors and accuracy using all of the information at their disposal.

Chapter B.2 describes the procedure to measure a single emission location that is emitting at an approximately constant rate. This is the default mode of operation, for the majority of emissions in the field. An additional operating mode is outlined in Chapter B.3 for time-varying sources.

B.2 Measurement of a Single, Constant, Source

This section describes the human-machine procedures for making a single high flow measurement, typically with several replicates, of an emission source that is emitting at a constant rate. The user is responsible for estimating that the emission rate is approximately constant.

Measurement is divided into two steps:

1) Auto-ranging concentration sensors.
2) Performing a measurement of emissions.

A typical high flow instrument may rely on multiple concentration sensors which are effective in different concentration ranges. This protocol is written as if there is more than one sensor and the instrument auto-selects between them to maximize the operating range of the instrument. However, some instruments may include only one sensor.

Note: The primary purpose of this process is to guard against several common measurement errors which often occur in field conditions, such as improperly capturing all of the leak emissions. The process is also intended to encourage the capture of multiple replicate measurements by providing a clear guide for automating the change in setpoints. This process will not guard against all errors, nor is it a substitute for proper training.

B.2.1 Auto-ranging

The intent of auto-ranging is to place one or more of the concentration sensors in the correct range for accurate measurement, and if that is not possible, to flag the user that the emission rate is outside the measurement capabilities of the instrument. The process is outlined in the flowchart at the right. Numbers indicate links into the measurement flowchart in Section B.2.2.

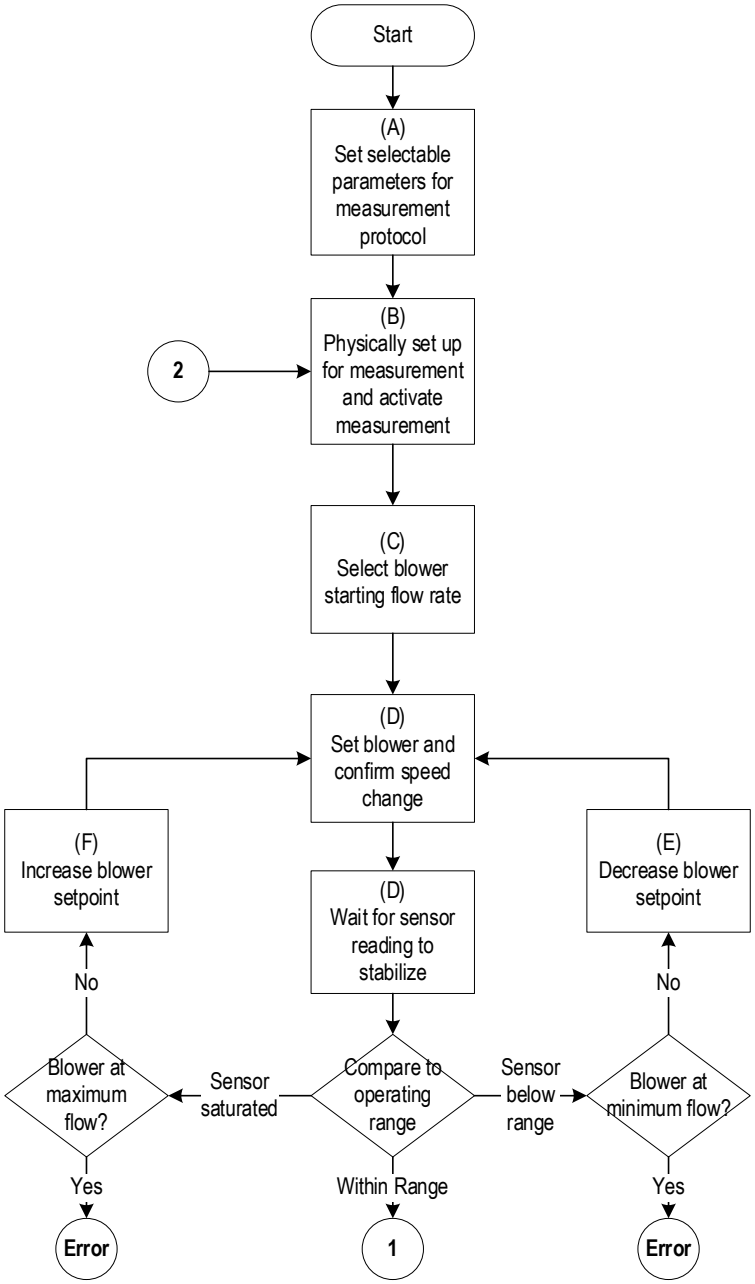

A. The user sets instrument parameters as defined in Section B.2.3.
B. User sets up the instrument and isolates the leak for measurement using the inlet hose, bag, or other device to enclose the leak; ensures the instrument is grounded; and completes any additional setup actions specified in the instrument manual. The user then initiates the auto-ranging process.
C. The instrument selects a starting blower speed as defined in (A).
D. Instrument sets the blower speed and reads sensors to ensure blower is operating as commanded. It then waits for the sensor readings to stabilize.
E. If all sensors are below range, the instrument decreases blower speed setpoint and loops to (D) to check adjustment. If blower is already at minimum flow rate, an error is generated, and measurement stops.
F. If all sensors are saturated, the instrument increases the blower speed setpoint and returns to (D). If the blower is already operating at maximum speed, an error is generated, and measurement stops.

When sensor(s) are operating within range, the instrument moves on to the measurement. Note that all data in A-F should be recorded for quality control purposes and marked as “auto-range”. In steps D-F, an advanced instrument may first attempt to auto-range so that multiple sensors are within usable range before defaulting to a single sensor.

B.2.2 Measurement

Measurement proceeds as in the next diagram. One *measurement* consists of *N* blower *setpoints,* each of which produces one calculated emission rate. Varying blower (air throughput) rates provides a check that the leak is being entirely captured for measurement.

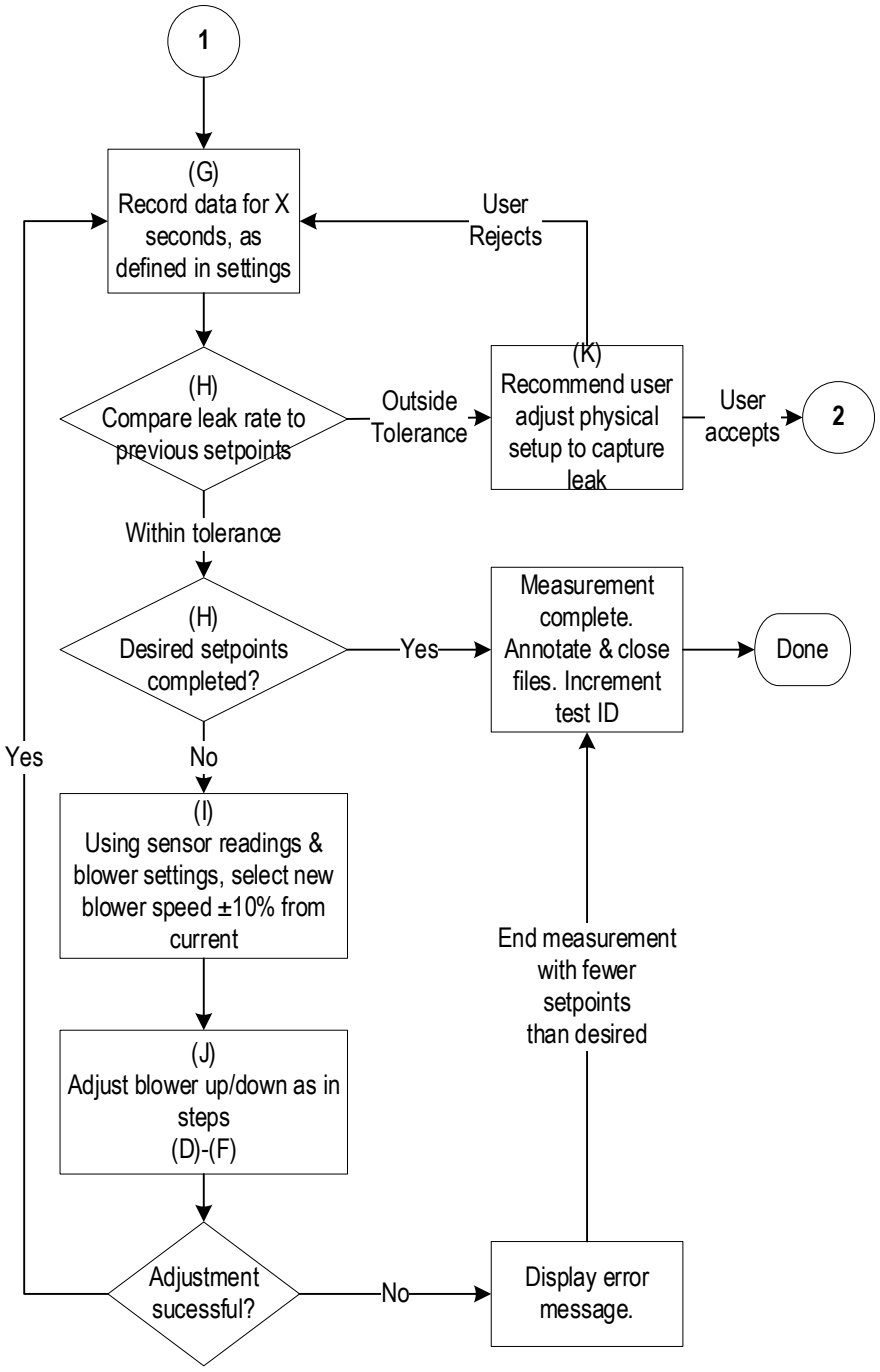

At the start of the measurement flowchart (at right), the instrument has auto-ranged and is capable of making a measurement. Therefore, the first step is to record data and calculate an emission rate for the starting setpoint.

G. The instrument records for a defined period, as specified in (A), completing one replicate of the measurement (one *setpoint*).

H. Instrument compares new setpoint to previous setpoints. If the measured leak rate is within tolerance ("emission rate tolerance" in Section B.2.3), the measurement setup has likely captured the entire leak. The instrument annotates and stores the results with appropriate quality indicators.

If enough setpoints have been completed, the measurement process is completed.

If the measured leak rate *is not* within tolerance, the leak may not be completely captured at this or prior setpoints. The instrument annotates and stores the results, marks them with a quality control indicator, and proceeds to step (K).

I. Comparing sensor(s) to their operating ranges, and blower to its operating range, instrument decides to raise or lower flowrate by desired amount (see "blower step fraction" in Section B.2.3).

J. Blower adjusts, with error conditions handled as in (D)-(F), above. If adjustment fails, an error message is displayed, and measurement completes with fewer setpoints than desired. If successful, return to (G) to complete setpoint.

K. If leak rate varies between setpoints in step (H), GUI recommends that the user check the physical capture of the leak. If guidance is accepted, flow returns to (2) on previous chart. If rejected, a quality control indicator is added to the measurement and the instrument continues with the next setpoint.

All data collected during this process is stored, and each setpoint is marked with quality control indicators.

The measurement completes normally (with no errors) when the desired number of replicates, that agree within the "emission rate tolerance" specified in Section B.2.3, have been acquired.

B.2.3 Setup Parameters

The above process accesses a set of configuration or setup parameters in the instrument (or if not automated, applied by the user) to complete a successful measurement. Additionally, a regulator or similar stakeholder may want to specify certain values for reported measurements to specify proper quality control.

The table below describes key parameters referenced elsewhere in this document. Recommend, minimum and maximum values are illustrative only. SBI ("set by instrument") indicates that either the instrument manufacturer, or the calibration procedure for the instrument, sets these values.

Parameter	Purpose	Recommended	Minimum Value	Maximum Value
Number of setpoints	Number of blower setpoints utilized to produce one complete measurement.	3	1	Any
Sensor usable range	Sensor readings are calibrated only in this range.	N/A	SBI	SBI
Blower usable range	Range of operational blower speeds.	N/A	SBI	SBI
Blower step fraction	What fraction of blower range to use to step blower speed up & down.	10 %	2-3 times the speed control resolution of the blower	N/A
Blower starting speed	Default blower speed in Step C. May be adjusted based upon common measurement tasks.	50 %	N/A	N/A
Emission rate tolerance between setpoints	Allowed variation between emission rates calculated by each blower setpoint.	±TBD (see note 1)	±10 %	±100 %
Sensor stability	Below this standard deviation of sensor reading, the sensor reading is considered stable (steps D or G).	±TBD (see note 1)	±1%	±100 %
Minimum setpoint time	Amount of time to record data after sensor is stable in Step G (averaging time).	15 s	1 s	120 s

Notes:
1) The expected stability of high flow measurements, in field conditions, needs to be characterized to set these values.

B.3 Time-Varying Sources

A time-varying source is an emission point that is expected to vary over the measurement time. Typical examples include venting from pneumatic controllers or devices, or emissions dependent on weather or pressure. Variability should not include changes in emission rate due to incomplete capture of the emission. Therefore, the user should utilize a secondary method, such as observation with an optical gas imaging (OGI) camera, to ensure all emissions are being captured.

Given sensor and blower response times, a typical instrument will not be able to auto-range during a measurement. Therefore, the user will select an appropriate blower speed that will maintain sensor readings within the sensor usable range for the portions of the measurement that are of interest.

For example, the blower may be set to capture peak emission rates of an intermittent source, at the expense of no reading during low emission periods.

In general, time-varying sources may not be automatically quantifiable by the instrument, although advanced instruments may be able to estimate and integrate emissions over time. Therefore, the primary emphasis of this measurement mode is to record data at the maximum speed supported by the instrument for post-recording analysis and emissions estimation. This places several requirements on the instrument:

1) The instrument will have documented time constants for the response time of all sensors.
2) The instrument will mark all recorded readings outside the sensor usable range with quality control indicators.
3) If readings between sensors are not simultaneous to within 1 % of the sampling rate of the instrument, the instrument will have documented offsets between sensor readings (concentration, total air flow rate, and environmental parameters like temperature and humidity).

Measurement process:

A. User sets up the instrument and isolates the leak for measurement using the inlet hose, bag, or other device to enclose the leak; ensures the instrument is grounded; and completes any additional setup actions specified in the instrument manual.
B. User configures blower speed and other parameters for continuous recording.
C. User verifies that all emissions are being captured at the selected settings.
D. User initiates recording.
    a. On each sample, instrument checks if sensors are within usable range (and other QC checks) and annotates sample with appropriate QC indicators.
    b. Over- and under-range indicators are shown on screen, but recording is not interrupted.
    c. If automatic, the instrument adjusts time delays between sensors to align measurement times.
    d. If automatic, the instrument provides a running average of total emissions.
E. User terminates recording after a pre-set interval. Recordings may range from a minute to many hours.
F. Instrument completes logging, annotates the recording, and increments the test ID.

In most cases, the user will later analyze recorded data to estimate emissions, emissions variability, and similar parameters.

Appendix C Testing Protocol

C.1 Introduction

In 2021 the CSU METEC team, working with partner SLR International, will conduct a performance test of existing and next-generation high flow samplers (HFSs), a common instrument type for measuring small leaks on gas equipment. This document outlines the protocol for the testing. Multiple HFS instruments will be tested during the study.

The objective of this testing is to understand the accuracy of the instruments in pseudo-realistic field conditions across each instrument's range of emission rates, at a variety of leak locations. Emission rates will be varied to map out the quantification curve from below the lower detection limit (LDL) to above the upper saturation limit (USL) or the safe maximum that can be released, whichever is lower.

Additionally, limited testing will include gas releases that contain higher fractions of ethane and propane to identify any issues with leak rate quantification.

All testing will be performed by an SLR or CSU engineer familiar with HFS use ("tester"). Testing will be white box to the tester – the tester will know where the leak is located, and (roughly) the emission rate – but black box to any observers from the HFS instrument companies. Multiple engineers may participate in testing; "tester" may refer to more than one person.

C.2 Publication

Data collected in this study will be published to CSU's web site and a journal paper or public report. It will also be provided to the California Air Resources Board as part of the deliverables for the project.

C.3 Test Facility

All testing will be performed at METEC using controlled releases from realistic emission locations. Locations will be located on wellheads, separators, compressors, a small dehydrator unit, and potentially tank thief hatches or vents, if available. It is not the objective of this testing to test every leak rate on every location. Rather, locations will be selected to identify issues with capture of all emissions.

Unless otherwise noted, emissions will be CNG gas, ranging from 85-95 % methane, with the balance primarily ethane. Gas composition will be ascertained using gas chromatography. Emission rates will be measured by installed gas flow meters at METEC; accuracy of these meters is well understood.

Emission rates will be varied from below the detection threshold of the instrument to either (a) saturation point of the instrument or (b) the safe operational limit for sampling. For LDL testing, the team will likely utilize a methane/nitrogen or methane/air mix to achieve very low emission rates.

C.4 Test Protocol

Testing will be divided into multiple phases or "test runs," each with a specific objective. In all cases, each HFS instrument will be used as instructed by the manufacturer, and data will be logged from the instrument's screen or electronically, as provided by the instrument. After the training period (see below) instrument manufacturers will not be allowed to manipulate or observe the test in any way, other than to repair, replace, or answer questions about the instrument.

C.4.1 Training

Each HFS company will provide up to one day of training to the tester prior to the study. This should be scheduled in advance directly with the tester. Backup testers may attend the training in case backups are necessary to cover the test time.

Prior to each day of testing, the tester will follow instructions to setup, check, and calibrate the instrument as per manufacturer's instructions. Notes will be taken to document startup procedures and note any anomalous behavior.

C.4.2 Test Run 1: Determine Instrument LDL on Methane

The purpose of this test is to determine the LDL of all instruments.

Location:

> Testing will be performed utilizing the mass flow controllers on the METEC gas mixing rig and for extremely low flows, critical orifices verified with DryCal volumetric provers. The release will be directed into the intake of the instrument. No enclosure or bagging of a leak location will be performed.

Test procedure:

1) Insert the leak pipe into the hose inlet of the instrument as specified by the instrument manufacturer.
2) Set the emission rate at the stated LDL of the instrument.
3) Allow emission rate to stabilize.
4) Record measurement results.
5) Lower emission rate and repeat (3) & (4), recording each measurement attempt, until the instrument consistently reports zero emissions or "no emissions detected".
6) Raise the emission rate above the LDL of the instrument until the instrument reports a non-zero measurement on each attempt. Record each measurement and measurement attempt for later analysis.

Expected results and analysis:

- Results of this experiment should map out the LDL response of each instrument in the form of a logistic curve between 0 % detection and 100 % detection. At minimum, there should be >2 recorded measurements at level(s) where emissions are *never reported* and >3 measurements at level(s) where non-zero emissions are always reported. An example is shown below. The example is for a BHFS tested as part of the GEF study. [25]

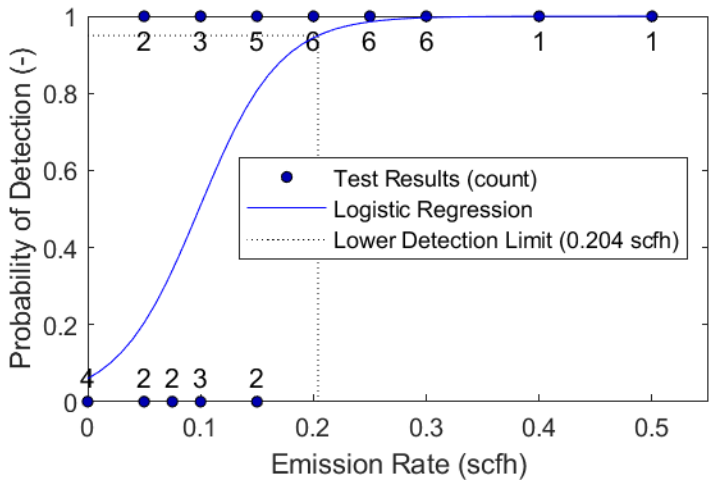

C.4.3 Test Run 2: Determine Instrument Accuracy

The purpose of this test is to map out the accuracy of each instrument across its stated measurement range.

Location:

Testing will be performed utilizing the gas mixing rig at METEC, with the release being directed into the intake of the instrument. Larger flow rates will be tested using metered releases from open ended-tubing or piping at METEC that are easily enclosed.

Test Procedure:

1) Tester will create a set of emission rates ranging from a level near the LDL determined in the previous test to the maximum rating of each instrument in the study. If the maximum flow rate cannot be achieved at METEC, or is not safe, the tester will select a maximum flow rate that can be implemented and note any deviation from the manufacturer's specifications in notes. Testing maximum rating will be performed on exposed piping that is easy to enclose ("bag") for sampling. The tester will select the location in consultation with METEC staff. Leak rates greater than 80 LPM will be performed with market gas and may be "bagged" if needed to ensure complete capture. Leak rates below 80 LPM will be performed using methane and tubing directed into the intake of the instrument.

Ten or more emission rates will be selected. Selected rates may be unevenly spaced if the team deems it necessary to cover the entire range of the instrument.

2) For each emission rate, the tester will:
    1. Remove all instruments from the leak location.
    2. Start the emissions at the desired rate.
    3. Following the instrument's protocol, enclose/capture the leak, and record a measurement.
    4. Record the emission rate from METEC equipment.
    5. Repeat until all instruments have been tested at the set rate. Randomize the order in which the instruments are utilized.

3) For approximately 25 % of the leak rates, the procedure in (2) will be repeated 2 additional times to provide a measure of repeatability for each instrument.

Expected Results and Analysis:

- Actual and reported emission rates will be compared on a XY plot to determine instrument accuracy both by emission rate bin and over the full operational range of the instrument.
- Repeatability will be similarly assessed.

C.4.4 Test Run 3: Determine Instrument Sensitivity to Gas Composition

The purpose of this test is to measure if emission rates reported by the instrument are impacted by a range of non-methane hydrocarbons in the emission stream.

Location:

All testing will be performed utilizing the gas mixing rig at METEC, with the release being directed into the intake of the instrument. No enclosure or bagging of a leak location will be performed.

Test Procedure:

1) Tester will create a matrix of wet gas compositions ranging from 30 % methane to 100 % methane, with varying dilution by ethane and propane. Approximately 7 gas mixtures will be selected.
2) For each selected gas mix:
    1. The tester will select an emission rate within the instrument's operational range, approximately 25 % of the way between LDL and USL.
    2. Allow instrument to stabilize at a zero reading in clear air.
    3. Insert the output of the gas mixing rig into the inlet of the instrument.
    4. Allow the measurement to stabilize.
    5. Record reading from instrument and reading(s) from gas mixing rig.

6. Remove gas outlet from instrument inlet.
7. Return to step 2 with different gas mix; repeat steps 2-6 to replicate the results.

3) During testing, record any error messages reported by the instrument.

Expected Results and Analysis:

- Analyze reported emission rates relative to gas mix, considering whether the instrument reports methane, total hydrocarbons, or other metric.

C.4.5 Test Run 4: Determine Instrument Sensitivity to Real World Measurement Locations

The purpose of this test is to determine how easily each instrument can accommodate emissions in non-ideal locations, such as within enclosures, large leak surfaces, etc.

Location:

Testing will take place at numerous locations around METEC that vary in complexity and accessibility. Locations will include, at a minimum:

- One location that has large outer diameter, such as the top casing ring on a wellhead.
- One large diameter source with low flow velocity, such as a thief hatch.
- One location that is structurally cumbersome to enclose, such as a valve actuator or pneumatic control box.

Test Procedure:

1) Tester will select five locations at METEC, as per the "location" list above.
2) Tester will select two emission rates for each instrument, one at 200 % of LDL, and one in the mid-range of the instrument's measurement range, as determined in Test Run 2. If the large rate is not possible, or if unsafe, at any location, the tester will use a reduced rate and note that in the experimental log.
3) For each emission rate/location combination:
    1. Allow instrument to stabilize at a zero reading in clear air.
    2. Bag or otherwise enclose the leak location as per manufacturer's instructions.
    3. Allow the measurement to stabilize.
    4. Record reading from instrument and METEC.
    5. Record qualitative observations on the ease/difficulty of making the measurement.
    6. Return to step 2 with other emission rate/location; repeat steps 2-5.
4) If possible, repeat steps in (3) three times for each instrument at each location and flow rate.

Expected Results and Analysis:

- Identify any deviation or difference, by instrument, of measuring in difficult locations, and any such dependency on the emission rate at the time of testing.

References

1. Zimmerle, D. J. *et al.* Methane Emissions from the Natural Gas Transmission and Storage System in the United States. *Environ. Sci. Technol.* **49**, 9374–9383 (2015).
2. Subramanian, R. *et al.* Methane Emissions from Natural Gas Compressor Stations in the Transmission and Storage Sector: Measurements and Comparisons with the EPA Greenhouse Gas Reporting Program Protocol. *Environ. Sci. Technol.* **49**, 3252–3261 (2015).
3. Lamb, B. K. *et al.* Direct Measurements Show Decreasing Methane Emissions from Natural Gas Local Distribution Systems in the United States. *Environ. Sci. Technol.* **49**, 5161–5169 (2015).
4. Allen, D. T. *et al.* Methane Emissions from Process Equipment at Natural Gas Production Sites in the United States: Pneumatic Controllers. *Environ. Sci. Technol.* **49**, 633–640 (2015).
5. Allen, D. T. *et al.* Methane Emissions from Process Equipment at Natural Gas Production Sites in the United States: Liquid Unloadings. *Environ. Sci. Technol.* **49**, 641–648 (2015).
6. DOE Announces $13 Million to Quantify and Mitigate Methane Emissions from Natural Gas Infrastructure. *Energy.gov* https://www.energy.gov/articles/doe-announces-13-million-quantify-and-mitigate-methane-emissions-natural-gas-infrastructure.
7. Integrated Component-Specific Measurements to Develop Emission Factors for Compressors and Reduce Uncertainties in the Greenhouse Gas Inventory | netl.doe.gov. https://www.netl.doe.gov/node/2219.
8. Vaughn, T. L. *et al.* Temporal variability largely explains top-down/bottom-up difference in methane emission estimates from a natural gas production region. *Proc. Natl. Acad. Sci.* 201805687 (2018) doi:10.1073/pnas.1805687115.
9. Roscioli, J. R. *et al.* Measurements of methane emissions from natural gas gathering facilities and processing plants: measurement methods. *Atmos Meas Tech* **8**, 2017–2035 (2015).
10. Lamb, B. K. *et al.* Development of Atmospheric Tracer Methods To Measure Methane Emissions from Natural Gas Facilities and Urban Areas. *Environ. Sci. Technol.* **29**, 1468–1479 (1995).
11. Conley, S. *et al.* Application of Gauss's theorem to quantify localized surface emissions from airborne measurements of wind and trace gases. *Atmospheric Meas. Tech.* (2017) doi:https://doi.org/10.5194/amt-10-3345-2017.
12. Harrison, M. R., Shires, T. M., Wessels, J. K. & Cowgill, R. M. *Methane Emissions from the Natural Gas Industry, Volume 1: Executive Summary*. 24 (1996).
13. Vaughn, T. L. *et al.* Comparing facility-level methane emission rate estimates at natural gas gathering and boosting stations. *Elem Sci Anth* **5**, (2017).
14. Bell, C. *et al.* Comparison of methane emission estimates from multiple measurement techniques at natural gas production pads. *Elem Sci Anth* **5**, (2017).
15. Zimmerle, D. J. *et al.* Gathering pipeline methane emissions in Fayetteville shale pipelines and scoping guidelines for future pipeline measurement campaigns. *Elem Sci Anth* **5**, (2017).
16. *Greenhouse Gas Reporting Program, Subpart W*. *Code of Federal Regulations*.
17. US EPA. *Method 21 - Determination of Volatile Organic Compound Leaks*. https://www.epa.gov/sites/production/files/2016-06/documents/m-21.pdf (2017).
18. Heath Consultants, Inc. Anti-Static Measurement Bag.
19. Bacharach Hi-Flow sampler, Instruction 0055-9017, Operation and Maintenance. (2015).
20. Howard, T. University of Texas study underestimates national methane emissions at natural gas production sites due to instrument sensor failure. *Energy Sci. Eng.* **3**, 443–455 (2015).
21. Howard, T., Ferrara, T. W. & Townsend-Small, A. Sensor transition failure in the high flow sampler: Implications for methane emission inventories of natural gas infrastructure. *J. Air Waste Manag. Assoc.* **65**, 856–862 (2015).

22. Alvarez, R. A., Lyon, D. R., Marchese, A. J., Robinson, A. L. & Hamburg, S. P. Possible malfunction in widely used methane sampler deserves attention but poses limited implications for supply chain emission estimates. *Elem Sci Anth* **4**, (2016).
23. *EPA Did Not Use Allegedly Flawed Studies to Estimate Methane Emissions or Set New Source Performance Standards for Oil and Natural Gas Production*. 19 (2018).
24. Connolly, J. I., Robinson, R. A. & Gardiner, T. D. Assessment of the Bacharach Hi Flow® Sampler characteristics and potential failure modes when measuring methane emissions. *Measurement* **145**, 226–233 (2019).
25. Zimmerle, D. *et al.* Methane Emissions from Gathering Compressor Stations in the U.S. *Environ. Sci. Technol.* **54**, 7552–7561 (2020).
26. GSI Environmental. *Draft Final Report: Quantification of Methane Emissions from Marginal (Small Producing) Oil and Gas Wells*. https://www.ipaa.org/wp-content/uploads/2022/01/Attachment-C-DOE_Draft-Final_Project-Report_31dec2021.pdf (2021).
27. Johnson, D. R., Covington, A. N. & Clark, N. N. Design and Use of a Full Flow Sampling System (FFS) for the Quantification of Methane Emissions. *JoVE J. Vis. Exp.* e54179–e54179 (2016) doi:10.3791/54179.
28. Tran, H. N. Q. *et al.* Emissions of Organic Compounds from Produced Water Ponds II: Evaluation of flux-chamber measurements with inverse-modeling techniques. *J. Air Waste Manag. Assoc.* **0**, null (2018).
29. Riddick, S. N. *et al.* Measuring methane emissions from abandoned and active oil and gas wells in West Virginia. *Sci. Total Environ.* **651**, 1849–1856 (2019).
30. Riddick, S. N., Mauzerall, D. L., Celia, M. A., Kang, M. & Bandilla, K. Variability observed over time in methane emissions from abandoned oil and gas wells. *Int. J. Greenh. Gas Control* **100**, 103116 (2020).
31. Deighton, J. A., Townsend-Small, A., Sturmer, S. J., Hoschouer, J. & Heldman, L. Measurements show that marginal wells are a disproportionate source of methane relative to production. *J. Air Waste Manag. Assoc.* **0**, null (2020).
32. Air Movement and Control Association. *AMCA 210: Laboratory Methods of Testing Fans for Ratings*. (1999).
33. AGA 3.1: Orifice Metering of Natural Gas and Other Related Hydrocarbon Fluids: Part 1. 66.
34. ISO 5167-1:2003 Measurement of fluid flow by means of pressure differential devices inserted in circular cross-section conduits running full.
35. ASTM E2029-11 Standard Test Method for Volumetric and Mass Flow Rate Measurement in a Duct Using Tracer Gas Dilution.